

Modelling of Low Flows in the North Esk River using the Macaque model

Final

for
Launceston City Council

MC Peel¹
FGR Watson²
RA Vertessy³

¹ The University of Melbourne, CRC for Catchment Hydrology

² California State University, Monterey Bay, CRC for Catchment Hydrology

³ CSIRO Land and Water, CRC for Catchment Hydrology

12 November 2002

Executive Summary

The water supply of the city of Launceston is sourced from the North Esk and St Patricks Rivers to the city's east. Water is supplied to Launceston directly from these rivers without the use of any water storage structures. Thus the level of summer low flows is critically important to the provision of water to Launceston. This project was initiated and managed by Steve Ratcliffe of the Launceston City Council Infrastructure Assets Division and funded by the Launceston City Council.

The North Esk and St Patricks catchments are covered in a mixture of native forest, private forest and pasture. Some of the native forest and all of the private forests comprise ash type eucalypt species (*E. regnans* or *E. nitens*) that yield more water when the forests are older than about 50 to 100 years old. The Kuczera curve was the first description of the relationship between water yield and age for ash type eucalypts (Kuczera, 1987). The Kuczera curve is an empirical relationship derived from water yield and forest age data collected over several decades. Macaque, a recently developed physically based spatial process model, has been largely successful in reproducing the Kuczera curve, for the Maroondah and Thomson catchments, using a process-based approach combining topography, climate, vegetation species and vegetation physiology relations.

In this project Macaque was applied to the North Esk catchment. The version of Macaque used in this project is very similar to the version applied to the Thomson catchment (Peel et al. 2000). Spatial data describing catchment elevation, vegetation type and vegetation age and time series data for runoff, precipitation and maximum and minimum temperature were collated. The data were processed into formats suitable for Macaque.

The major aims of this project were to,

- 1) accurately simulate the historical streamflow record of the North Esk River (particularly the low flows) using Macaque,
- 2) investigate the source areas of low flows for the North Esk River,
- 3) assess the level of impact that changes to the distribution of vegetation age and type will have on the low flows of the North Esk River.

Macaque was successfully calibrated against runoff data for the North Esk River at the Ballroom for the period 1/1/1950 – 31/12/1969. The calibrated Macaque was also run from 1/1/1970 – 31/12/1998 as a verification of the model. The verification results indicate the possibility of unrecorded changes in the vegetation type or age in this period that was not modelled. Flow duration curves were also used to compare the observed and modelled runoff for the calibration and verification periods. The modelled lowest 40% of flows were on average 12% less than the observed for the calibration period.

Four logging rotation scenarios were simulated using a synthetic climate. The synthetic climate is daily data from a climatically average year, 1962, repeated to form a long time series. The synthetic climate has no inter-annual variability so the simulated effects on water yield are due to the modelled changes in vegetation age and species. The logging rotations modelled were 100-year, 50-year and 20-year logging rotations of areas covered in *E. regnans* and a 20-year rotation of areas covered in *E. regnans* and pasture, which was progressively converted to *E. nitens* (tree farm). Total runoff and low flows were affected least in the 100-year logging rotation scenario and most in the 20-year logging rotation and tree farm scenario. The range of mean daily flow impact of the scenarios was a reduction of 3% for the first rotation of the 20-year logging rotation to a 33% reduction for the second rotation of the 20-year logging rotation and tree farm scenario. The range of impact on the lowest 40% of flows was a 4% reduction for the first rotation of the 20-year logging rotation scenario to a 25% reduction for the 20-year logging rotation and tree farm scenario. Considering that the lowest 40% of flows were 12% lower than the observed in the calibration, the 20-year logging rotation and tree farm scenario second rotation low flows are significantly lower than the calibrated runoff.

A catchment wide fire scenario was also modelled using the synthetic climate. The maximum impact on water yield occurred eight years after the fire. The maximum impact of the fire scenario on mean daily flow was a reduction of 44% and the lowest 40% of flows were reduced by 50% relative to the observed data.

The source areas of modelled total runoff and low flows were investigated in a climatically average year. Areas covered in E. regnans and grassland account for 73% of the catchment area and produce 54.7% of the total runoff and 33.5% of the runoff in the three driest months (low flows). The modelled impact of the logging rotation scenarios on low flows is smaller than the modelled impact on mean daily runoff due to the modified areas of the catchment contributing a smaller proportion of runoff for low flows than for total runoff.

The impact on water yield of the 20-year rotations is greater than that of the 100-year rotation, due to the difference in resultant average forest age, LAI and water yield. The 20-year rotation forest (average age of 10) has higher values of LAI and thus lower water yield than the 100-year rotation forest (average age of 50).

The potential impact on total runoff and low flows of the same logging rotation, tree farm and fire scenarios on the St Patricks catchment is likely to be similar to that modelled in the North Esk since the St Patricks catchment has a smaller area of E. regnans and grassland, but also a smaller area of heath and rock.

The range of possible flows is strongly related to climate variability and only weakly related to vegetation changes associated with logging scenarios. However, the location of the range of possible flows is influenced by vegetation changes associated with logging scenarios.

The main limitation of the project was the quality of the vegetation type and vegetation age data. Several other limitations were noted but these are mainly issues for further research and model improvement.

Considering the limitations of some of the model input data, the results achieved with Macaque in this project are very good. The spatial and temporal dynamics elucidated by the model for the various logging rotation scenarios are far more detailed than any previous analyses conducted in this area of work. Most other studies of catchment response to forest logging have focused on mean annual yield impacts at a lumped catchment level. The ability of Macaque to predict responses down to the daily and Hillslope level gives catchment managers considerable insight into how different logging regimes would impact on water resources in different ways.

Acknowledgments

The assistance of the following people is gratefully acknowledged.

Steve Ratcliffe of the Launceston City Council Infrastructure Assets Division for initiating and managing the project. Cameron Oakley of the same division for assisting Steve Ratcliffe in the management of the project.

Hector Beveridge, Alex Crothers and Julian Ward of the Launceston City Council Spatial Information team for collating and converting the spatial data into a format suitable for Macaque.

Martin Stone from Forestry Tasmania for providing the vegetation location and age maps.

Andy Warner from Private Forests Tasmania for providing vegetation location and age class data for private forests in the North Esk and St Patricks catchments.

Bruce Stewart, Jim Elliot, Chris MacGeorge and Kevin Smith from the Bureau of Meteorology for providing daily precipitation, maximum and minimum temperature data.

David Fuller from DPIWE Tasmania for providing the streamflow data for the North Esk River at the Ballroom. Mark Willis and David Wilson from HEC Tasmania and Ross James from the Bureau of Meteorology for providing streamflow data for the St Patricks River at Nunamara.

Joel Rahman from the CSIRO Land and Water, CRC for Catchment Hydrology for help with Macaque.

Table of Contents

| | | |
|-------|--|----|
| 1. | Introduction | 6 |
| 1.1 | FOREST WATER YIELD AND SUMMER LOW FLOWS..... | 6 |
| 1.2 | AIMS | 7 |
| 1.3 | REPORT OUTLINE..... | 7 |
| 2. | The Catchments..... | 8 |
| 2.1 | INTRODUCTION | 8 |
| 2.2 | NORTH ESK CATCHMENT | 8 |
| 2.2.1 | <i>North Esk River at the Ballroom</i> | 8 |
| 2.3 | ST PATRICKS CATCHMENT | 9 |
| 2.3.1 | <i>St Patricks River at Nunamara</i> | 9 |
| 3. | Macaque | 10 |
| 3.1 | INTRODUCTION | 10 |
| 3.2 | MODEL STRUCTURE..... | 10 |
| 3.3 | DATA REQUIREMENTS | 11 |
| 3.3.1 | <i>Topographic</i> | 11 |
| 3.3.2 | <i>Vegetation</i> | 12 |
| 3.3.3 | <i>Precipitation</i> | 16 |
| 3.3.4 | <i>Temperature</i> | 19 |
| 3.4 | FIXED PARAMETERS | 20 |
| 4. | Model calibration on the North Esk catchment | 22 |
| 4.1 | INTRODUCTION | 22 |
| 4.2 | CALIBRATIONS | 22 |
| 4.3 | FLOW DURATION CURVES | 25 |
| 4.4 | CONCLUSIONS | 27 |
| 5. | Predicting water yield impacts of logging rotation scenarios in the North Esk catchment | 28 |
| 5.1 | INTRODUCTION | 28 |
| 5.2 | DATA AND METHODOLOGY | 28 |
| 5.3 | SIMULATION RESULTS | 29 |
| 5.4 | DISCUSSION | 36 |
| 5.5 | APPLICATION TO ST PATRICKS CATCHMENT | 38 |
| 5.6 | CONCLUSION..... | 39 |
| 6. | Predicting water yield impacts of logging rotation scenarios in the North Esk catchment under a variable climate | 41 |
| 6.1 | INTRODUCTION | 41 |
| 6.2 | DATA AND METHODOLOGY | 41 |
| 6.3 | SIMULATION RESULTS | 41 |
| 6.4 | CONCLUSION..... | 43 |
| 7. | Limitations | 45 |
| 7.1 | INTRODUCTION | 45 |
| 7.2 | DATA AVAILABILITY | 45 |
| 7.3 | MODEL UNCERTAINTY | 45 |
| 7.4 | UN-MODELLED PROCESSES | 45 |
| 8. | Conclusion | 46 |
| 9. | References | 48 |
| A. | Appendix (Flow duration curve values)..... | 50 |
| B. | Appendix (Species annual evapotranspiration)..... | 52 |

1. Introduction

1.1 Forest Water Yield and Summer Low Flows

The water supply of the city of Launceston is sourced from the North Esk and St Patricks Rivers to the city's east. Water is supplied to Launceston directly from these rivers without the use of any water storage structures. Thus the level of summer low flows is critically important to the provision of water to Launceston. This project was initiated and managed by Steve Ratcliffe of the Launceston City Council Infrastructure Assets Division and funded by the Launceston City Council.

The North Esk and St Patricks catchments are covered in a mixture of native forest, private forest and pasture. Some of the native forest and all of the private forests comprise ash type eucalypt species (*E. regnans* or *E. nitens*) that yield more water when the forests are older than about 50 to 100 years old. This higher water yield is because evapotranspiration (ET) from older forests is lower per unit area than from younger forests. The implication is then that forest disturbance by fire or logging reduces water yield in the short to medium term (except in the few years immediately after disturbance). The relationship between catchment disturbance and catchment water yield has been established by an extensive programme of experimental and analytical research, initially by the then Melbourne Metropolitan Board of Works (now Melbourne Water), and more recently by the Cooperative Research Centre for Catchment Hydrology. Recent summaries were given by Vertessy et al. (1994 & 1998) and Watson et al. (1999a).

One of the main conclusions of this work, a water yield versus forest age relation, was described by Kuczera (1987). This relation was developed from rainfall and runoff data collected from large forested catchments that were completely or partially burnt by a large-scale wildfire in 1939. The 'Kuczera curve' (Figure 1.1) predicts a decline in water yield immediately after clearing, leading to a minimum at about 20 to 30 years, followed thereafter by a gradual rise back toward 'old-growth' water yield at about 100 years of age. More recently, Watson et al. (1999a) derived a similar curve based on rainfall and water yield data from smaller paired experimental catchments. The new curve shows similar characteristics to the Kuczera curve, differing mainly by predicting a sharp initial increase in water yield before the decrease introduced by Kuczera.

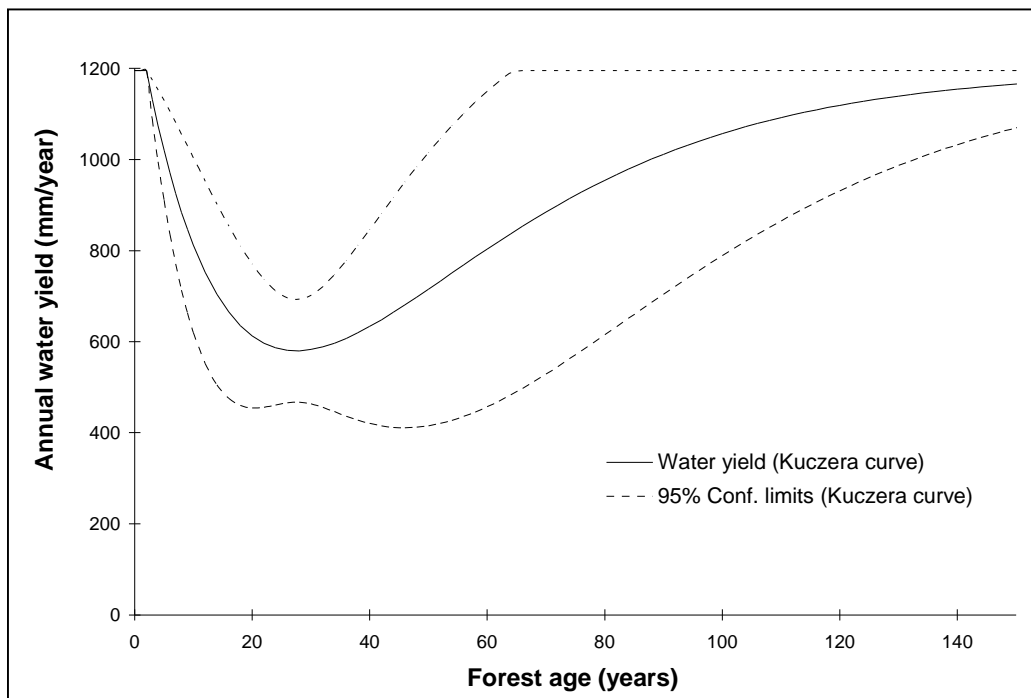


Figure 1.1 Annual water yield versus forest age (Kuczera Curve) from Watson et al. (1999a).

Watson (1999) developed a spatially distributed process model, named Macaque, which, for the first time, reproduced the water yield versus time since disturbance relationship described by Kuczera (1987), using methods which were sensitive to spatial and temporal variations in forest type and forest age. The Macaque model was developed and tested using data from the Maroondah catchments.

In this project Macaque will be applied to the North Esk catchment in order to address the following project aims.

1.2 Aims

The major aims of this work are to:

- Accurately simulate the historical streamflow record of the North Esk River (particularly low flows) using Macaque.
- Investigate the source areas of low flows for the North Esk River.
- Assess the level of impact that changes to the distribution of vegetation age and type will have on the low flows of the North Esk River.

1.3 Report Outline

Section 2 describes the catchment and data used in this report and is followed by a section outlining the Macaque model and its data requirements. The Macaque model is applied and calibrated for the North Esk catchment in Section 4. Four potential logging rotation scenarios and a catchment wide fire scenario are simulated in Macaque and the results analysed in Section 5. One of the potential logging rotation scenarios is re-modelled under different conditions in Section 6. The limitations of the project are briefly presented in Section 7. Conclusions drawn from this research project are presented and discussed in Section 8.

2. The Catchments

2.1 Introduction

This section contains some descriptive information about the North Esk and St Patricks catchments. Initially the St Patricks catchment was to be modelled, however there was insufficient good quality daily streamflow records for the St Patricks River to allow a modelling analysis. Thus this section is largely devoted to descriptions of the North Esk catchment.

2.2 North Esk catchment

The North Esk river is located to the east of Launceston, in the state of Tasmania, Australia. Water is supplied to Launceston from this catchment. The topography of the North Esk catchment is steep and mountainous, ranging from 20m to 1570m above sea level. Mean annual precipitation ranges from 800mm to 2300mm across the catchment. The catchment has a mixture of land uses, mainly native forest and pasture with some heath, rocky outcrops and plantations. In drier regions, dry sclerophyll species such as Messmate (*E. Obliqua*), Manna (*E. viminalis*) and Swamp Gum (*E. ovata*) are observed. Wet sclerophyll forests are found between 400m and 800m and these predominately consist of Mountain Ash (*Eucalyptus regnans*) and Alpine Ash (*E. delegatensis*). At higher elevations Snow Gum (*E. pauciflora*) and Tasmania Snow Gum (*E. coccifera*) are found and above 1200m is generally alpine scrubland (personal communication Pat O'Shaughnessy, 2001). The catchment geology is largely Ordovician mudstone and Devonian granodiorite. Tertiary basalt forms the peaks of Ben Lomond, Ben Nevis and Mount Barrow. There are also small areas of Holocene alluvial, Triassic sandstone, Pleistocene sediments and late Carboniferous glaciomarine mudstone (McClenaghan & Calver, 1994).

The North Esk River at the Ballroom is the only streamflow gauge considered, since this was the only gauging station with a good quality long-term daily record.

2.2.1 North Esk River at the Ballroom

The catchment area of the North Esk River at the Ballroom is 367 km² (36730 ha). Daily streamflow records were available from 20/4/1923 through to 19/10/1999 with 0.07% of the period of record being estimated and 2.30% missing.

The location of the gauging station relative to Launceston is shown in Figure 2.1. The North Esk catchment referred to in the remainder of this report is defined as the North Esk catchment above the gauging station at the Ballroom.

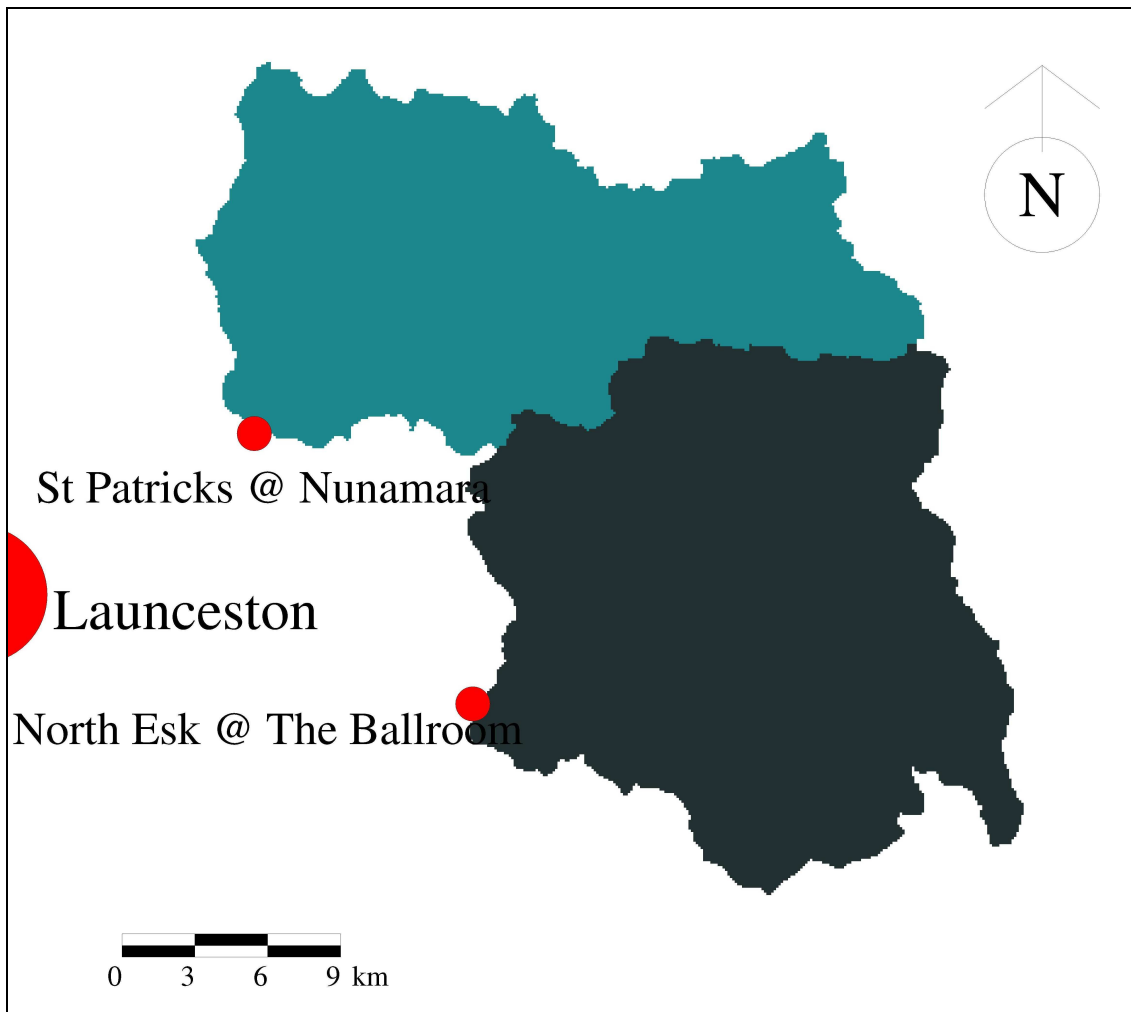


Figure 2.1 Location of North Esk at the Ballroom and St Patricks at Nunamara gauging stations and catchment areas relative to Launceston, Tasmania.

2.3 St Patricks catchment

The St Patricks River is located to the east of Launceston, in the state of Tasmania, Australia and to the north of the North Esk catchment. Water is supplied to Launceston from this catchment. The topography of the St Patricks catchment is less steep and mountainous than the North Esk catchment, ranging from 225m to 1390m above sea level. The catchment has a mixture of land uses, mainly native forest and pasture with some rocky outcrops and plantations. The distribution of species is similar to that found in the North Esk catchment.

The St Patricks River at Nunamara is the only streamflow gauge considered, since this was the only gauging station with a good quality daily record in the St Patricks catchment.

2.3.1 St Patricks River at Nunamara

The catchment area of the St Patricks River at Nunamara is 296 km² (29650 ha). Daily streamflow records were available from 15/11/1991 through to 9/8/1994 with 0% of the period of record being estimated and 0% missing.

The location of the gauging station relative to Launceston is also shown in Figure 2.1. With less than three years of daily data available, the St Patricks at Nunamara streamflow record is of insufficient length to be used in the following modelling analysis. The St Patricks catchment referred to in the remainder of this report is defined as the St Patricks catchment above the gauging station at Nunamara.

3. Macaque

3.1 Introduction

The Macaque model was developed by Watson (1999 and Watson et al. 1998 & 1999b) at the Cooperative Research Centre for Catchment Hydrology. The structure of Macaque and its data requirements are outlined in this section.

3.2 Model Structure

This section is largely a reprint of a similar section in Peel et al (2000) with minor additions.

The model is physically based, meaning that it aims to represent the dominant, real physical processes occurring within a catchment using mathematical equations. This approach is intended to offer predictive capability in situations where measurements of water yield have not been taken, in a way that is sensitive to estimated spatial and temporal changes in climate, topography, and land cover. As much as possible, the many parameters of the model have been given values based on direct measurements of physical properties at Maroondah, or on reasonable values taken from the literature. A few parameters, particularly those relating to soil properties, are left for calibration against observed water yield. Such parameters are unlikely to change with forest disturbance. Once they are calibrated for a given catchment under known disturbance regimes, they are considered to be robust. Therefore, model predictions are considered to be valid when future disturbance regimes are specified.

A complete model description was given by Watson (1999), with summaries given by Watson et al. 1998 & 1999b. The structure and operation of Macaque is described briefly here.

The model splits catchments spatially into hillslopes, and hillslopes into smaller areas called elementary spatial units (ESUs). Each ESU is modelled separately and these are each linked together by subsurface water flow pathways. Hillslopes are linked together by a stream network, which simply adds up the flow from all the hillslopes to get the total catchment flow. The model runs on a daily timestep and requires a daily time series of precipitation and maximum and minimum temperature for input.

Within each ESU, two layers of vegetation are represented: canopy and understorey. Precipitation falls through these layers and can be intercepted by them. Radiation is also propagated through, and absorbed by these layers. The Penman-Monteith equation (Monteith & Unsworth, 1990) is used to calculate evapotranspiration (ET) from each of the layers, as well as evaporation from the soil.

Each ESU has two soil zones, representing unsaturated and saturated soil respectively. The interface between these is the water table, which moves up and down in response to vertical water movement, and inflows and outflows from and to ESUs above and below within the hillslope. The Van Genuchten model (Van Genuchten, 1980 & Rawls et al. 1993) is used to calculate recharge from the unsaturated to the saturated zone. Darcy's Law (Shaw, 1994) is used to move saturated water laterally within hillslopes using explicit transfers of water between neighbouring ESUs. This last step is a new development and differs from the original model presented by Watson (1999), which used an implicit lateral subsurface water distribution routine governed by a 'distribution function'. The new explicit scheme was tested when applied to several catchments by Peel (1999) and Peel et al. (2000). The evolution of the explicit scheme is described in Watson et al. (2001).

A detailed climate sub-model is used to convert precipitation and temperature range inputs into other climate variables such as radiation and humidity.

Predictions of water yield are sensitive to climate, plant water use, the amount of water stored within the soil, and the rate at which this water moves into and out of the soil to the streams. Therefore, spatial changes in climate, plants, soil, and topography causes changes in water yield.

Changes in forest type and age are represented by changes in leaf area index (LAI) and leaf conductance to water vapour. These are specified to the model as a series of LAI/age and conductance/age curves for each forest type (e.g. Mountain Ash, Mixed Species, Scrub, Open water).

The model is programmed in C++ and runs on IBM-compatible PCs under the Tarsier visual modelling framework (Watson, 2000).

3.3 Data Requirements

Macaque requires several spatial and temporal data sets. These requirements include topographic, vegetation and climate data, details for which are outlined below.

3.3.1 Topographic

A digital elevation model (DEM) is used to define catchment boundaries and delineate hillslopes and ESUs. It is also the source of topographic parameters, such as slope, aspect, and elevation, which are used to compute solar radiation, amongst other things. The resolution of the DEM used is constrained by data availability, as well as the catchment size and the speed of the computer that will be running the model. In this report a 100m by 100m DEM was used in preference to the 25m by 25m DEM, due to speed considerations and the size of the catchment. The North Esk DEM was provided by Launceston City Council and is shown in Figure 3.1.

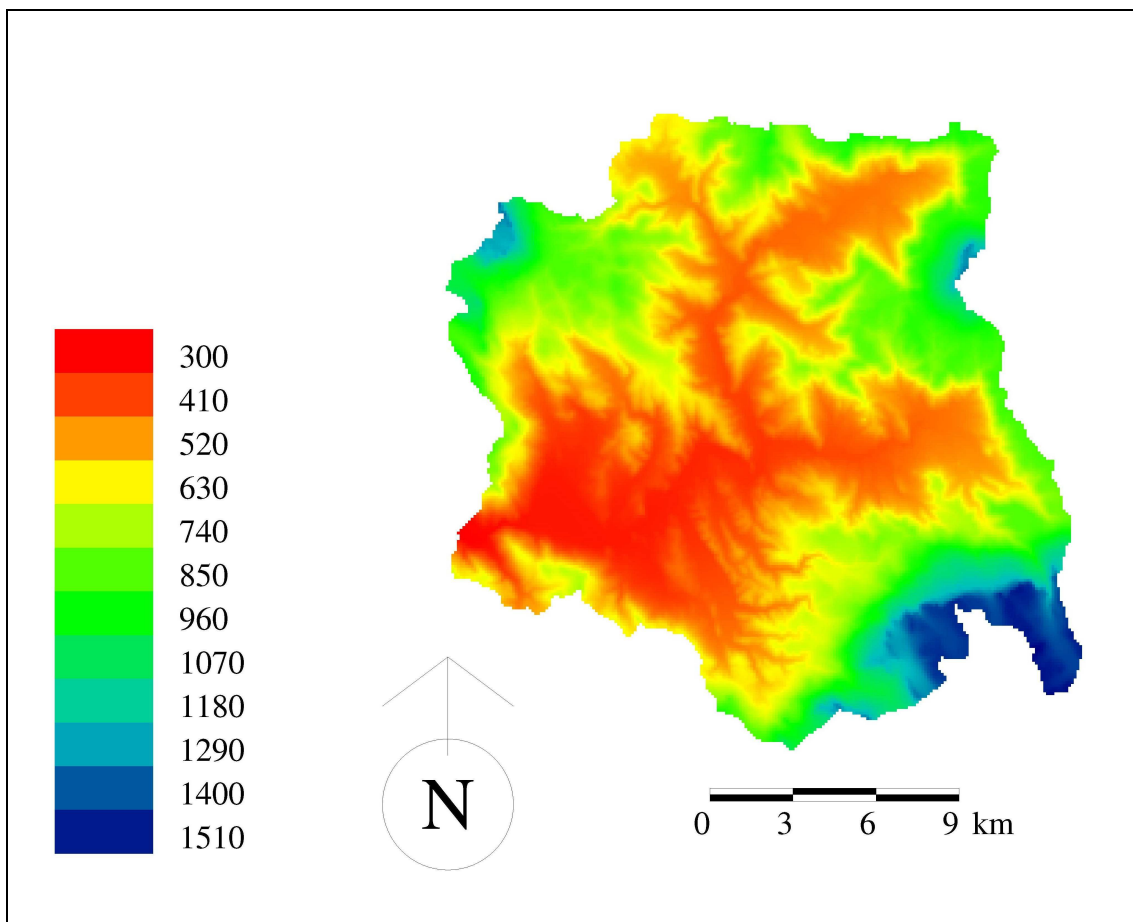


Figure 3.1 Digital elevation model, in metres (m), of the North Esk at the Ballroom catchment.

Once the resolution of the DEM has been selected, the DEM is analysed to determine the catchment boundary and the hillslopes and ESUs that are required for model operation. The DEM is analysed in the following manner.

- Pits and flats in the DEM are removed using the algorithm of Watson (1999).

- A stream network is calculated and hillslopes are identified as the area upslope of each segment of the network (Figure 3.2).
- A topographic index (Beven et al., 1995) is calculated at all points in the DEM. This index increases as one moves down the hillslope, and decreases as the terrain steepens.
- Areas of similar topographic index are grouped together as single ESUs within each hillslope.
- A location for the bottom of the catchment is selected and all hillslopes and ESUs upstream of this point are included in that catchment.

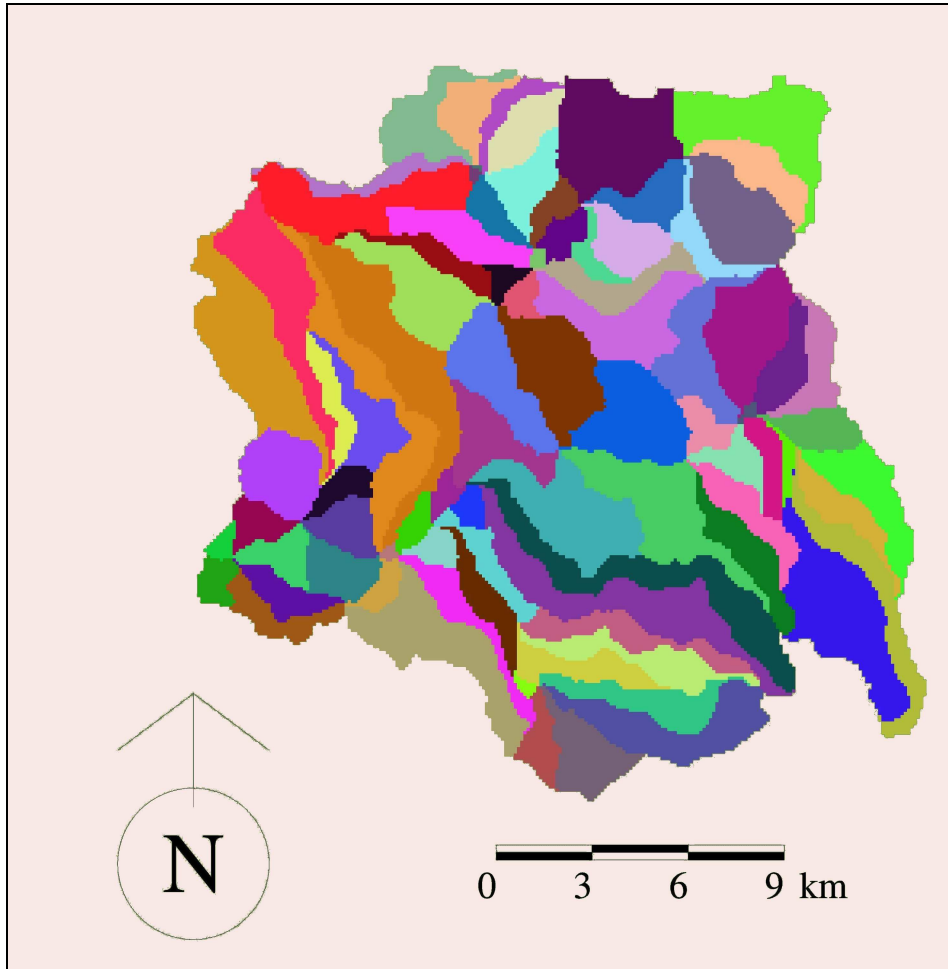


Figure 3.2 Randomly colored hillslope map of the North Esk at the Ballroom catchment.

3.3.2 Vegetation

Macaque requires forest type and forest age information in order to operate. A map of forest type (Figure 3.3a) was provided by Forestry Tasmania for the North Esk catchment. The forest type map was modified in order to infill missing data and sub-divide the “non forest” category into “grassland”, “rocky” and “heath” (Figure 3.3b). The infilling of missing data and the sub-division of the “non forest” category was conducted with reference to the vegetation age map (Figure 3.4) and an estimate of Leaf Area Index (LAI) derived from satellite imagery (Figure 3.6). Figure 3.3b was further modified by the inclusion of a small area of private forests, the location of which was provided by Private Forests Tasmania.

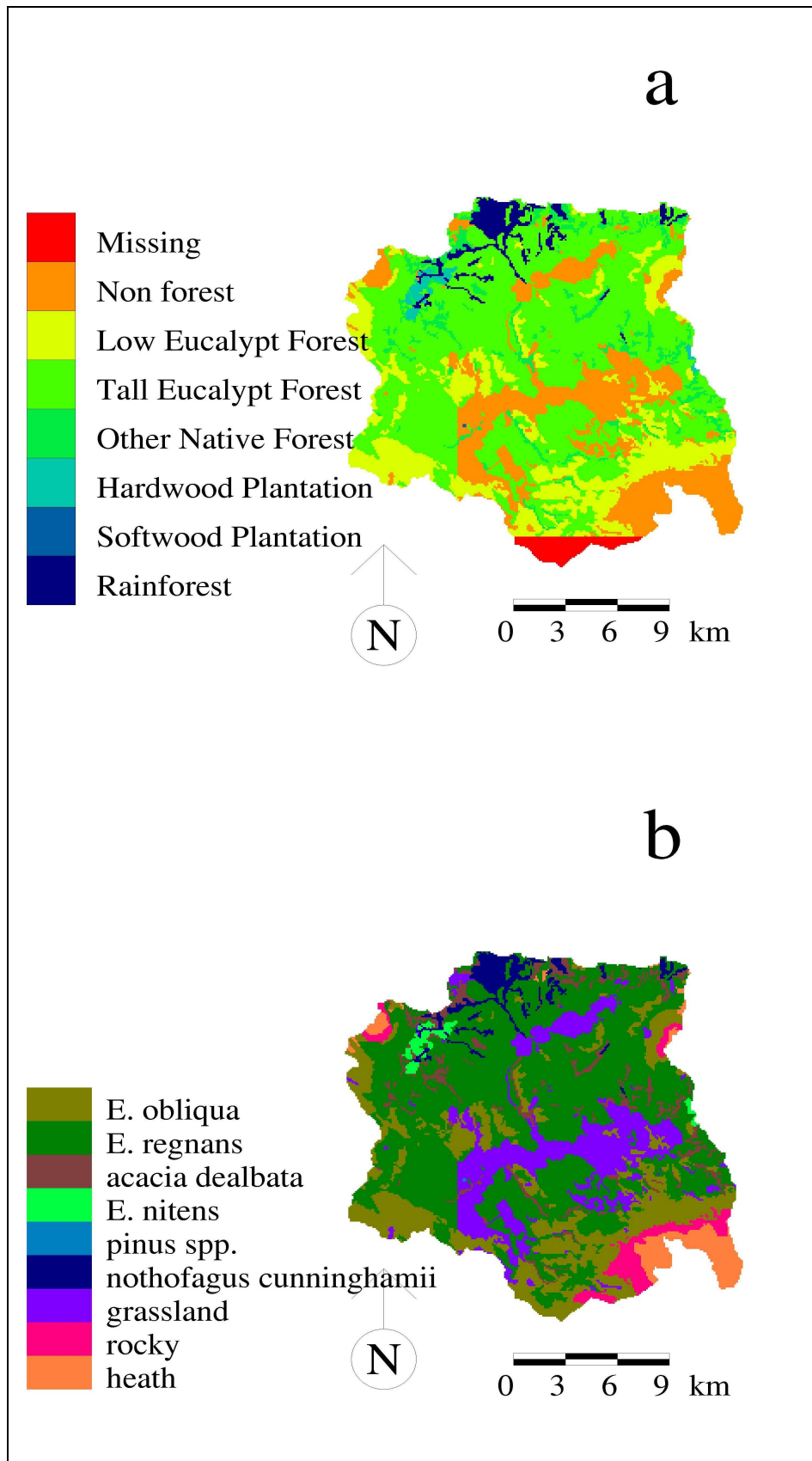


Figure 3.3 (a) Vegetation type map for the North Esk catchment as provided by Launceston City Council. (b) Modified vegetation map of the North Esk.

The broad categories of forest type in Figure 3.3a are not applicable to Macaque so particular species were assigned to each broad category (Figure 3.3b). Thus “low eucalypt forest” is represented in

Macaque as Messmate (*E. obliqua*), “tall eucalypt forest” by Mountain Ash (*E. regnans*), “other native forest” by Silver Wattle (*Acacia dealbata*), “hardwood plantation” by Shining Gum (*E. nitens*), “softwood plantation” by a generic pine species, “rainforest” by Myrtle Beech (*Nothofagus cunninghamii*) and “non-forest” by a combination of grassland, rocky and heath. Private forests are represented by Shining Gum.

Forestry Tasmania and Private Forests Tasmania provided vegetation age data. This data was combined to form a map of vegetation age for the North Esk catchment (Figure 3.4). The age classes 1985-1989, 1990-1994 and 1995-1999 were supplied by Private Forests Tasmania and refer to private hardwood plantations (*E. nitens*). Forestry Tasmania supplied the remaining vegetation age classes.

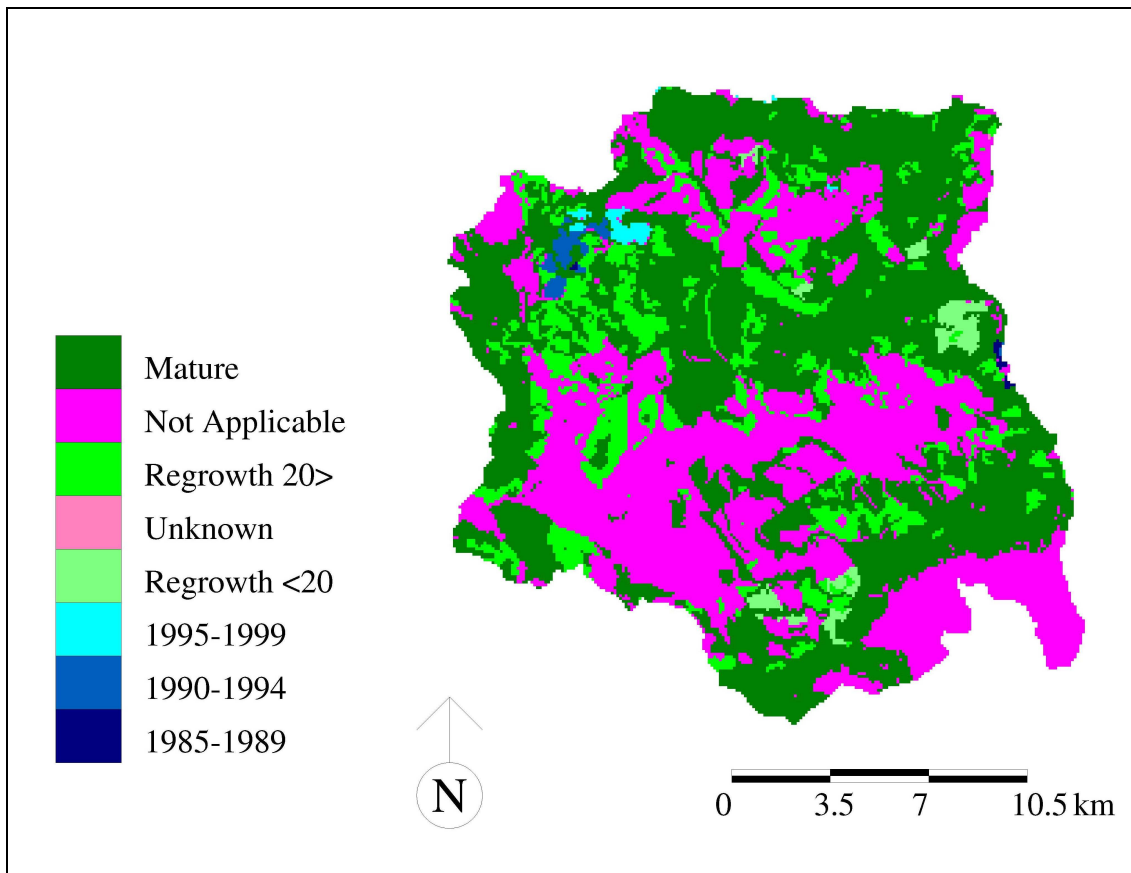


Figure 3.4 Vegetation age map for the North Esk catchment.

Whether the forest type has changed over the last 200 years from that observed today is unknown. The forest has been logged over time, but precise records as to when and where were not available. The fire history of the catchment was also unavailable. Maps of vegetation disturbance dates were created for the catchment. Since the precise dates of disturbances are unknown an initial disturbance in 1800 is assumed to be the first disturbance of the North Esk catchment. The date of 1800 was chosen in order to make the native forest mature during the modelling period.

No other major disturbance is assumed to have occurred. Regrowth that is older than 20 years is assumed to be the result of logging activity that is assumed to have occurred in 1945. Regrowth that is younger than 20 years is also assumed to be due to logging activity and is assumed to have occurred in 1985. The private plantations were assumed to be disturbed in 1800 and then in 1987, 1992 and 1997 for the 1985-1989, 1990-1994 and 1995-1999 age classes respectively.

The above assumptions about forest type, age and disturbance were required in order for the model to run. However, they are also indicative of a lack of knowledge about the forest type and age structure of the forests in the North Esk catchment. This lack of knowledge means that the margin for error in the modelling analysis is increased, as the assumptions made may be incorrect.

Macaque also requires information on long-term vegetation development. These are supplied in the form of curves for each species representing changes in LAI and leaf conductance with forest age. Of primary interest here are curves for *E. regnans* because this is the species which is known to cause long term changes in water yield as a result of changes in LAI and leaf conductance (Watson, 1999; Watson et al., 1999b, Vertessy et al. 2000). Figure 3.5 shows the LAI versus age curve for *E. regnans* from 0 years (disturbance) to 250 years after disturbance. The other ash-type species are also of key interest, because they are here assumed to follow the same LAI and leaf conductance patterns as *E. regnans*. These species include *E. delegatensis* and *E. nitens*. Little is known of long-term LAI trends in forests dominated by non-ash species. They are here assumed to have constant LAI, following a rapid initial increase from zero in the first 5 to 10 years following clearing. Following the work of Roberts et al. (2000), a long-term decline in leaf conductance is assumed to hold for all eucalypt forests, including non-ash species. This is a fairly significant assumption, based on limited evidence. Its impact is revealed later in this report, and serves to illustrate the importance of future work aimed at elucidating the long-term growth dynamics of Australia's forests. Table 3.1 summarises the LAI and leaf conductance dynamics assumed for each species here.

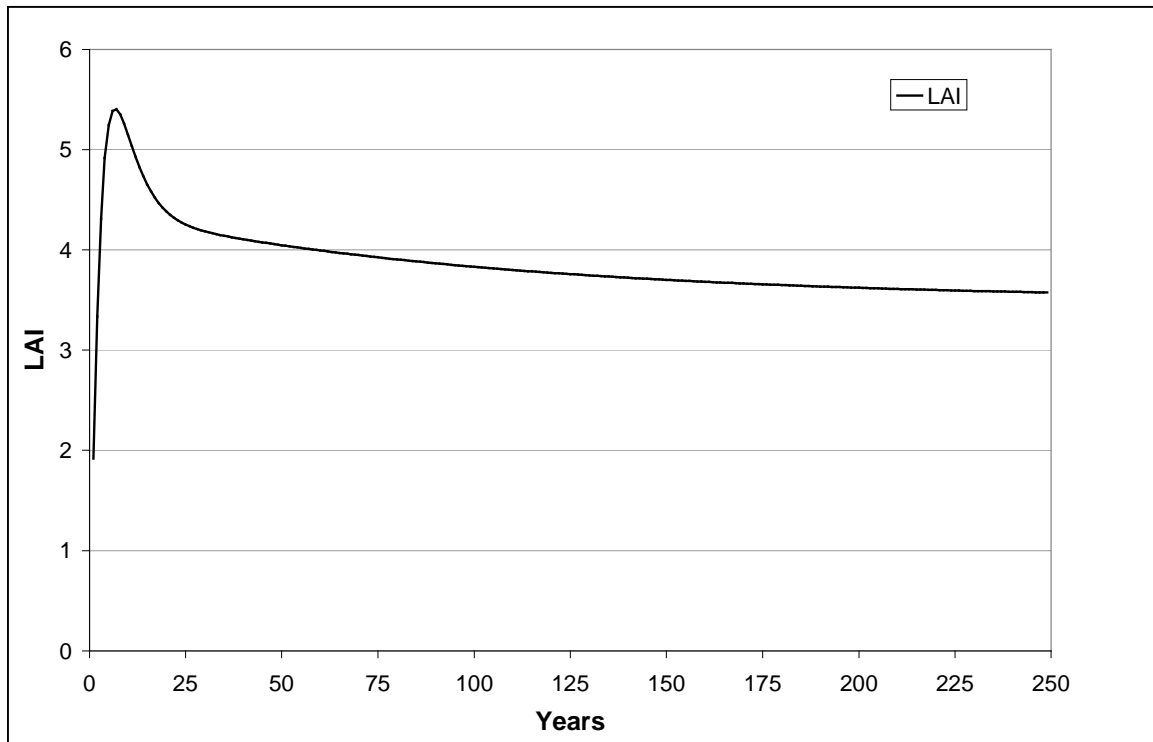


Figure 3.5 Annual ESU LAI versus age curve for *E. regnans* for the first 250 years after disturbance (from Peel et al., 2000).

Table 3.1

Long-term trends in leaf area index (LAI) and maximum leaf conductance assumed for the vegetation types present at North Esk.

| Forest type | LAI curve type | Maximum LAI | Long-term LAI | Leaf conductance curve type |
|--------------------------------|----------------------------|-------------|---------------|-----------------------------|
| <i>Acacia dealbata</i> | Constant* | 3.907 | 3.907 | Watson (1999) ³ |
| <i>E. delegatensis</i> | Watson (1999) ² | 5.7 | 3.2 | Watson (1999) ³ |
| <i>E. nitens</i> | Watson (1999) ¹ | 6.0 | 3.5 | Watson (1999) ³ |
| <i>E. obliqua</i> | Constant* | 2.5 | 2.5 | Watson (1999) ³ |
| <i>E. regnans</i> | Watson (1999) ¹ | 6.0 | 3.5 | Watson (1999) ³ |
| <i>Nothofagus cunninghamii</i> | Constant* | 4.5 | 4.5 | Watson (1999) ³ |
| Heath | Constant* | 1.5 | 1.5 | |
| Grassland | Constant* | 1.5 | 1.5 | |
| Rocky | Constant | 0.5 | 0.5 | |

* Constant after first 5 to 10 years of initial establishment, ¹ Watson (1999), Equation 8.45. Also, Watson et al. (1999b), ² Watson (1999), Equation 8.45. Also, Watson et al. (1999b). Same as ¹ but with LAI lower by 0.3, ³ Watson (1999), Equation 11.1. Also, Watson et al. (1999b).

Values of total LAI used in modelling the North Esk were assigned to each vegetation type according to our experience gained in the Maroondah and Thomson catchments. Field measurements of LAI for comparison with modelled values were not available. Assessment of whether the modelled total LAI values were accurate in terms of magnitude could not be assessed without field measurements; however, remote sensing was used to assess whether the spatial variability of modelled total LAI was realistic.

Remote sensing of the electro magnetic spectrum reflected from vegetation can be used to construct measures of vegetation density, called vegetation indices. Watson (1999) reviewed numerous vegetation indices and noted that the most popular index is the normalized difference vegetation index (NDVI) originated by Rouse et al. (1973, 1974). Using NDVI, Baret et al. (1989, cited by Lacaze, 1996) presented a formula for the transformed NDVI (TNDVI) that can be calibrated to directly predict LAI. TNDVI values were calculated from Landsat TM images taken on the 4/2/1998 provided by the Launceston City Council. The TNDVI values were then converted into estimates of LAI using the calibration method outlined in Watson (1999). Because field measurements of LAI were not available, TNDVI could not be calibrated against known LAI values for the North Esk. Therefore, TNDVI could not be used to assess the accuracy of the modelled LAI values. However, it could provide some insight into the spatial variability of modelled LAI. Figure 3.6 displays the difference between remotely sensed LAI and modelled total LAI for the North Esk on the 4/2/1998. Regions of green are where modelled total LAI is greater than remotely sensed LAI, while regions of red are where remotely sensed is greater than modelled LAI. The largest difference between modelled and remotely sensed LAI is found in the west of the catchment where modelled LAI is higher than the remotely sensed LAI. This over estimate of LAI by the model is most likely due to an error in the map of vegetation type (3a & b), the vegetation type indicated and modelled is *E. regnans*, when it perhaps should be grassland.

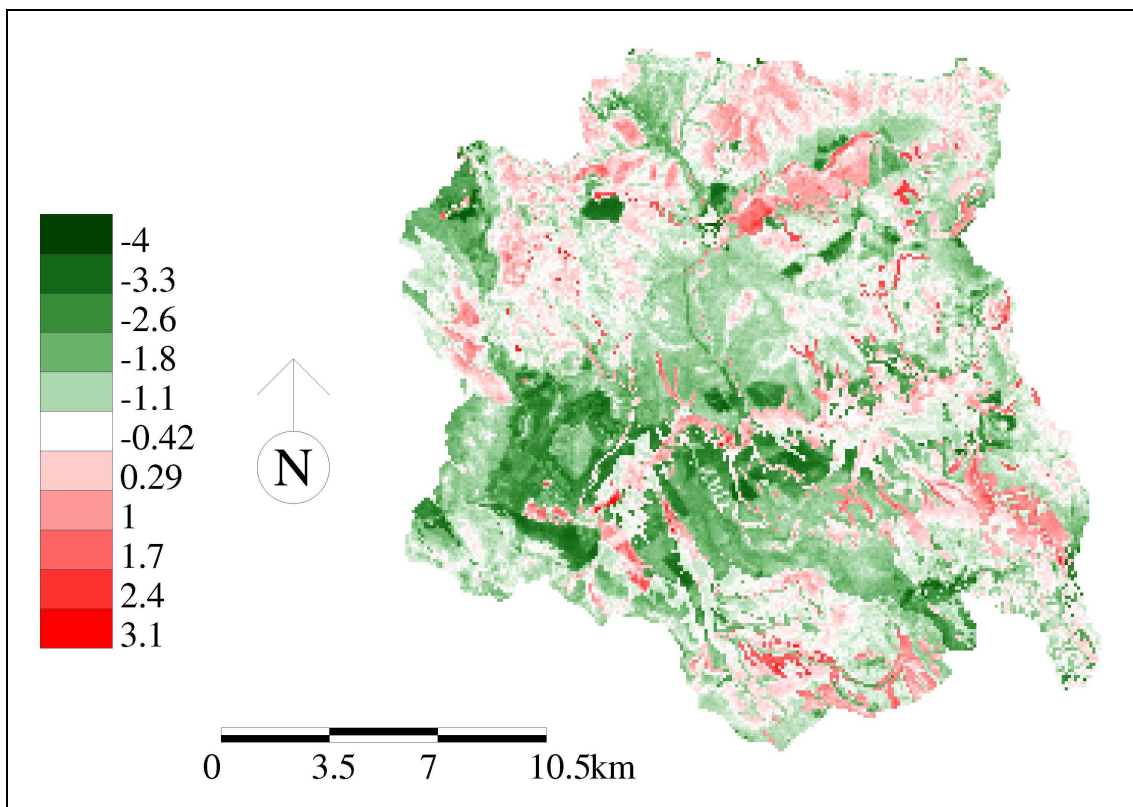


Figure 3.6 Difference between remotely sensed and modelled LAI for the North Esk catchment on 4/2/1998.

3.3.3 Precipitation

The Macaque model requires an estimate of precipitation at each ESU every day in order to run. Since observed daily precipitation values are not available at every ESU, a method of producing estimates of daily precipitation at each ESU is required. Peel et al. (2000) assessed two methods; the mean monthly

precipitation index (MMPI) method developed and used by Watson (1999) and the multiple linear regression (MLR) method developed and tested as part of Peel et al. (2000). The MLR method was found to improve objective measures of model performance by approximately 10% compared to the MMPI method (Peel et al., 2000). The MLR method incorporates more of the spatial variability of precipitation than the MMPI method and will be used through out this report.

The MLR method is based on a single multiple linear regression of the monthly precipitation at many stations against the monthly precipitation at a small number of base stations.

The steps involved in the MLR method are as follows:

1. Select multiple daily precipitation stations that have long continuous periods of record, near the catchment, as base stations (for the North Esk, three are used).
2. Convert all the precipitation records into monthly time series (gaps are allowed)
3. At each station
 - Conduct a multiple linear regression of the observed monthly precipitation against the base stations, with a zero intercept.
4. For each base station, interpolate a map (3-D spline) of the MLR coefficient corresponding to that base station (in this case, three maps).
5. Calculate the averages of each coefficient with each ESU.
6. Run the model
7. As the model runs, it calculates the daily precipitation of the ESU as the sum of the product of the daily precipitation at each base station with that base station's (fixed) coefficient for that ESU.

Precipitation data from 42 stations in and around the North Esk catchment were used in the MLR rainfall mapping analysis. The Bureau of Meteorology provided the daily precipitation records. The location of the forty-two precipitation stations is shown in Figure 3.7. The stations are listed along with some details about each time series in Table 3.2.

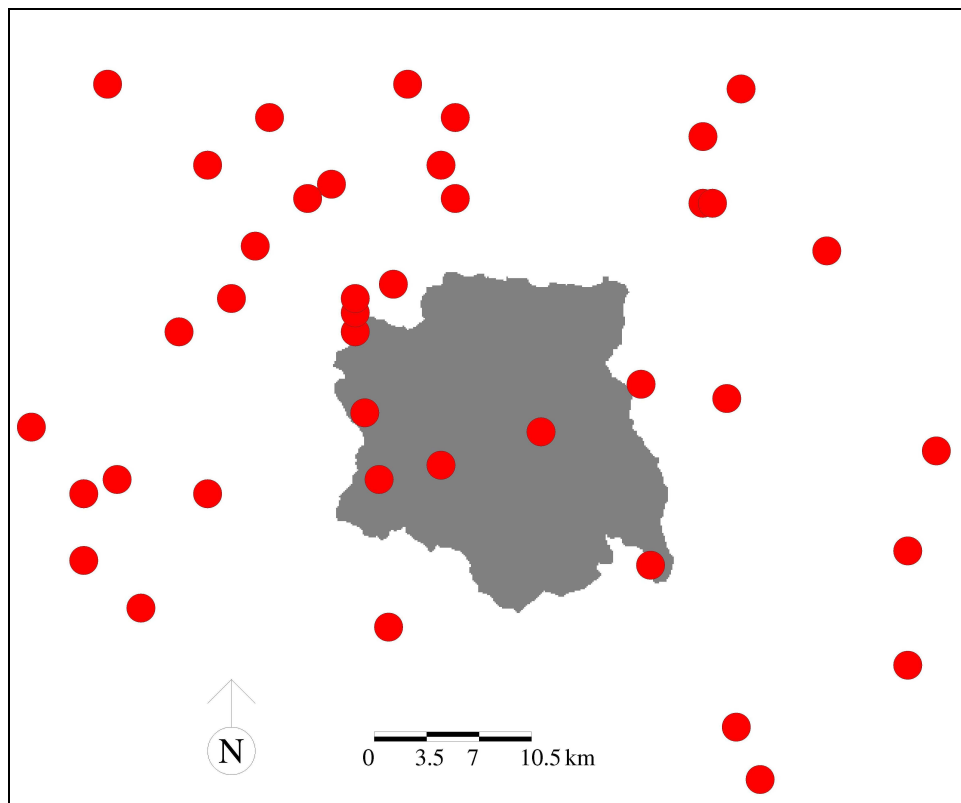


Figure 3.7 Location of precipitation stations in and around the North Esk catchment.

Table 3.2

Location and details of the precipitation stations used in the MLR analysis. Abbreviations: BOM ID is the identification number of the Bureau of Meteorology record.

| Name | BOM ID | Easting (m) | Northing (m) | Elevation (m) |
|-------------------------------------|---------------|-------------|--------------|---------------|
| Musselboro (Applico) | 91068 | 535918 | 5411410 | 381 |
| Mount Barrow | 91131 | 535109 | 5416965 | 1322.8 |
| Musselboro (Elverton) | 91197 | 536730 | 5406965 | 380 |
| Mt. Barrow (South Barrow) | 91198 | 535115 | 5418075 | 1320 |
| Mount Barrow (Hec No 1) | 91199 | 535120 | 5419185 | 1310.6 |
| Musselboro (View Banks) | 91200 | 535918 | 5411410 | 460 |
| Burns Creek (Janefield) | 91225 | 540911 | 5408053 | 400 |
| Upper Blessington (Combined) | 92004 + 92081 | 547604 | 5410232 | 460 |
| Ben Lomond | 92098 | 555053 | 5401298 | 1465 |
| Diddleum Plains | 91026 | 541848 | 5425811 | 633 |
| Dunne Creek | 91028 | 558623 | 5430136 | 255 |
| Launceston (Pumping Station) | 91049 | 516693 | 5405929 | 24.4 |
| Lilydale (Post Office) | 91053 | 518433 | 5433679 | 160 |
| Myrtle Bank (Lanoma) | 91069 | 529316 | 5431423 | 520 |
| Launceston (King Meadows) | 91072 | 513363 | 5410377 | 67 |
| Nunamara | 91075 | 523406 | 5417012 | 350.5 |
| Deddington (Nile River) | 91077 | 537513 | 5396969 | 275 |
| Evandale (Ridgeside) | 91084 | 525040 | 5405905 | 85.3 |
| Ringarooma (Fry Street) | 91086 | 561163 | 5433445 | 280 |
| St Patricks River(Trout Creek Farm) | 91088 | 528444 | 5422545 | 380 |
| South Springfield | 91093 | 541880 | 5431362 | 270 |
| Tayene | 91098 | 537634 | 5420283 | 643 |
| Launceston Airport | 91104 | 516683 | 5401489 | 170 |
| Evandale | 91118 | 520844 | 5398147 | 165 |
| Patersonia North | 91188 | 525116 | 5428108 | 426.7 |
| Mount Victoria (Mt Albert Rd) | 91194 | 566926 | 5422292 | 790 |
| Nunamara (St Patricks River) | 91202 | 526758 | 5419221 | 425 |
| Weelatya | 91254 | 538541 | 5433600 | 220 |
| Trenah (Wattle Banks) | 91257 | 558587 | 5425695 | 330 |
| Corra Linn (North Esk River) | 91263 | 519200 | 5407033 | 40 |
| Targa (Camden Road) | 91264 | 533483 | 5426964 | 430 |
| Diddleum (Sowers Road) | 91270 | 541024 | 5428036 | 635 |
| Targa (Priors Road) | 91305 | 531804 | 5425862 | 440 |
| Trenah (Gum Flat Road) | 91308 | 559424 | 5425688 | 332 |
| Rossarden (Aberfoyle) | 92000 | 562435 | 5386804 | 610 |
| Mangana | 92023 | 572503 | 5394481 | 270 |
| Mathinna (Fingal Road) | 92024 | 574319 | 5408897 | 285 |
| Tower Hill | 92042 | 572581 | 5402253 | 427 |
| Roses Tier (Memory Road West) | 92083 | 554311 | 5413516 | 870 |
| Rossarden | 92090 | 562435 | 5386804 | 597 |
| Upper Esk (Millybrook) | 92096 | 560150 | 5412359 | 360 |
| Storys Creek (Storys Creek Rd) | 92100 | 560798 | 5390149 | 779.2 |

Three base stations were selected for the MLR analysis. These were the stations at Upper Blessington (Combined), St Patricks River (Trout Creek Farm), and Launceston Airport. Two Upper Blessington stations (Blessington Upper (BOM ID = 92004) and Upper Blessington (Heathcote) (BOM ID = 92081)) were joined together to provide a third long term precipitation time series.

Missing data was infilled for each of the three base stations by simple linear regression with nearby daily precipitation gauges. The percentage of total record infilled for each base station was 0.47% (Launceston Airport), 4.43% (St Patricks River (Trout Creek Farm)) and 11.42% (Upper Blessington Combined).

The location of each precipitation station is known in three dimensions (easting, northing and elevation), therefore a 3-D spline can be used to interpolate the MLR coefficients across the entire catchment. The result of this process is a number of maps (equal to the number of base stations used) that represent the MLR coefficients of each base station at all locations. Figure 3.8 presents the MLR maps for the North Esk.

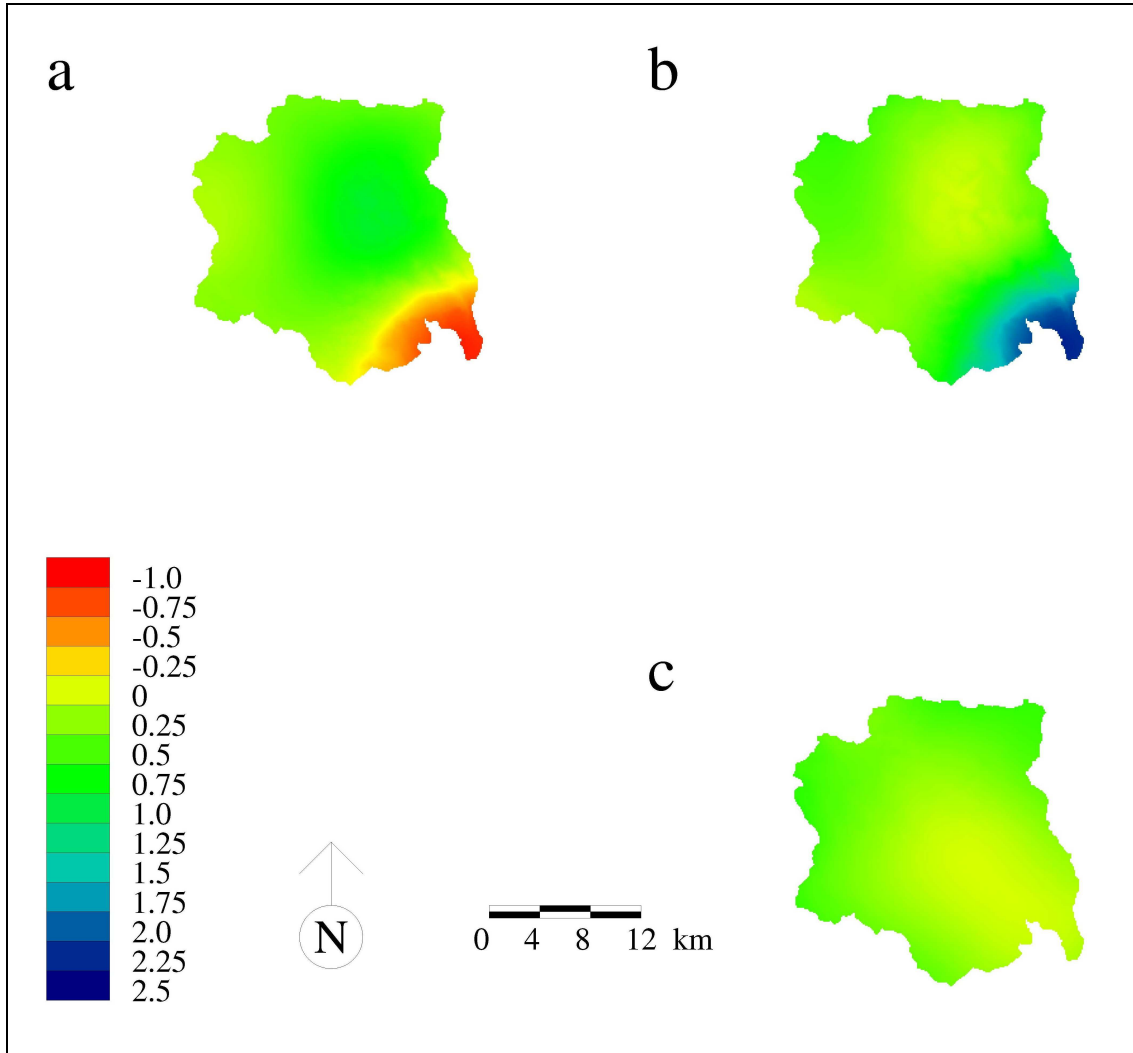


Figure 3.8 MLR coefficient maps for (a) Upper Blessington combined, (b) St Patricks River (Trout Creek Farm) and (c) Launceston Airport precipitation station.

The quality of the MLR fit to the observed data has yet to be tested and this issue requires further research. Ideally a split-sample, cross-validation test would be employed, whereby the MLR was performed a number of times on a number of stations for a certain period leaving out a single station each time. The method would be then used to predict precipitation at each excluded station in turn, using base station data from a period different to that used in the original regression.

3.3.4 Temperature

Daily maximum and minimum temperature data are also required for each ESU for each time step. As such data is only available for a few points within the catchment, a method of estimating maximum and minimum temperatures across space is required. As in Watson (1999), we used elevation-based lapse rates to calculate maximum and minimum temperatures at a given ESU from a base station from the difference in elevation between the ESU and base station. The temperature at a given ESU was calculated according to Equation 1.

$$T_{ESU} = T_{BS} + (\Gamma_x \times \Delta_{Elev}) \quad (1)$$

In Equation 1, T_{ESU} represents the temperature at an ESU (in °C), T_{BS} represents the temperature at the base station (in °C), Γ_x represents the lapse rate (either for maximum or minimum temperature in °Cm⁻¹) and Δ_{Elev} represents the change in elevation (in meters). This equation was applied for both maximum and minimum temperature at each ESU.

The Bureau of Meteorology provided maximum and minimum temperature data. The temperature gauge at Launceston Airport provided the longest and most complete record in the North Esk area and is used as the temperature base station in this report. The lapse rate for maximum and minimum temperature between Launceston Airport and the catchment was determined by comparing the maximum and minimum temperature records for gauges around the catchment, particularly those at higher elevations, with that at Launceston Airport. Important temperature gauges were located on Mont Barrow and Ben Lomond (although only a few months of data). The comparison results (not shown) indicate that a maximum temperature lapse rate of 0.008 °Cm⁻¹ and a minimum temperature lapse rate 0.0045 °Cm⁻¹ are the most appropriate lapse rates to use and these are used throughout the report.

3.4 Fixed parameters

Macaque uses numerous parameters that are fixed in space and time, which are described in detail by Watson (1999). Parameter names and values used in the present study are listed in Table 3.3 for reference.

Table 3.3
Macaque model parameters and values used for this report.

| Model parameter name | Fixed value | Comments |
|--|-------------|-------------------------------|
| p_elevation | variable | From DEM map data |
| p_sin_aspect | variable | From DEM map data |
| p_cos_aspect | variable | From DEM map data |
| p_slope | variable | From DEM map data |
| p_mean_monthly_precipitation_index | variable | From MMPI map data |
| p_precipitation_scalar | variable | Calibration parameter |
| p_precipitation_coeff_0 | variable | From MLR map data |
| p_precipitation_coeff_1 | variable | From MLR map data |
| p_precipitation_coeff_2 | variable | From MLR map data |
| p_precipitation_coeff_3 | variable | From MLR map data |
| p_precipitation_coeff_4 | variable | From MLR map data |
| p_precipitation_coeff_5 | variable | From MLR map data |
| p_max_temperature_elevation_lapse_rate | 0.006 | |
| p_min_temperature_elevation_lapse_rate | 0.006 | |
| p_bristow_and_campbells_a | 0.766 | |
| p_bristow_and_campbells_b | 0.0327 | |
| p_bristow_and_campbells_c | 1.46 | |
| p_origin_1 | variable | From vegetation age map data |
| p_origin_2 | variable | From vegetation age map data |
| p_origin_3 | variable | From vegetation age map data |
| p_rain_interception_coeff | 0.0008 | |
| p_snow_interception_coeff | 0.0008 | |
| p_slope_leaf_water_potential_vs_rel_water_availability | -100000 | |
| p_minimum_leaf_conductance | 0.0002 | |
| p_slope_leaf_cond_vs_cold_temp | 0.0002 | |
| p_slope_rel_leaf_cond_vs_warm_temp | 0.0003 | |
| p_canopy_species | variable | From vegetation type map data |
| p_canopy_radiation_extinction_coeff | 0.37 | |
| p_canopy_reflection_coefficient | 0.19 | |
| p_canopy_root_depth | 4 | |
| p_canopy_leaf_water_potential_at_stomatal_closure | -2300000 | |

| | | |
|--|----------|-----------------------|
| p_canopy_leaf_water_potential_maximum | -500000 | |
| p_maximum_canopy_leaf_conductance | 0.005 | |
| p_slope_canopy_relative_leaf_cond_vs_vpd | 0.0003 | |
| p_canopy_leaf_conductance_radiation_threshold | 0 | |
| p_canopy_reference_aerodynamic_resistance | 15 | |
| p_sat_canopy_transpiration_proportion | 0.1 | |
| p_canopy_leaf_conductance_radiation_parameter | 100 | |
| p_canopy_leaf_conductance_max_temperature | 40 | |
| p_canopy_leaf_conductance_optimal_temperature | 25 | |
| p_canopy_leaf_conductance_min_temperature | 0 | |
| p_min_temperature_causing_stomatal_closure | -8 | |
| p_intercept_canopy_leaf_conductance_vs_lwp | -2000000 | |
| p_shape_canopy_leaf_conductance_vs_lwp | 400000 | |
| p_canopy_leaf_conductance_vpd_factor | 0.0007 | |
| p_canopy_co2_for_max_leaf_conductance | 350 | |
| p_canopy_co2_causing_stomatal_closure | 1050 | |
| p_slope_soil_resistance_vs_vwc | -15000 | |
| p_soil_resistance_vwc_threshold | 0.2 | |
| p_atmospheric_co2_concentration | 350 | |
| p_understorey_radiation_extinction_coeff | 0.93 | |
| p_understorey_species | -1 | |
| p_understorey_reflection_coefficient | 0.13 | |
| p_understorey_root_depth | 2 | |
| p_understorey_leaf_water_potential_at_stomatal_closure | -2300000 | |
| p_understorey_leaf_water_potential_maximum | -500000 | |
| p_maximum_understorey_leaf_conductance | 0.005 | |
| p_slope_understorey_relative_leaf_cond_vs_vpd | -0.0003 | |
| p_understorey_leaf_conductance_radiation_threshold | 0 | |
| p_understorey_canopy_aerodynamic_resistance | 15 | |
| p_sat_understorey_transpiration_proportion | 0.5 | |
| p_snow_reflection_coefficient | 0.65 | |
| p_min_snowpack_degree_days | -30 | |
| p_snowmelt_coeff_temperature | 0.001 | |
| p_snowmelt_coeff_rad | 0.12 | |
| p_soil_reflection_coefficient | 0.1 | |
| p_soil_understorey_aerodynamic_resistance | 15 | |
| p_evaporation_depth | 0.003 | |
| p_soil_evaporation_tortuosity_factor | 2 | |
| p_water_reference_aerodynamic_resistance | 75 | |
| p_water_reflection_coefficient | 0.05 | |
| p_surface_saturated_hydraulic_conductivity | variable | Calibration parameter |
| p_minimum_saturated_hydraulic_conductivity | variable | Calibration parameter |
| p_saturated_hydraulic_conductivity_shape | variable | Calibration parameter |
| p_saturated_hydraulic_conductivity_depth | variable | Calibration parameter |
| p_ratio_hydraulic_to_surface_gradient | variable | Calibration parameter |
| p_saturated_volumetric_water_content | 0.67 | |
| p_residual_volumetric_water_content | 0.2 | |
| p_van_genuchten_n | 1.8 | |
| p_clay_fraction | 0.15 | |
| p_sand_fraction | 0.35 | |
| p_field_capacity_volumetric_water_content | 0.45 | |
| p_irrigation_threshold | 0.85 | |

4. Model calibration on the North Esk catchment

4.1 Introduction

In this section, the Macaque model is calibrated for the North Esk catchment. The data required to conduct the calibration were outlined in Section 3.3. The calibration results are presented and discussed. A comparison between the observed flow duration curve and that of the calibrated flow duration curve is also presented and discussed.

4.2 Calibrations

The Macaque model was applied to the North Esk using a daily time step and calibrated against daily streamflow data. The calibration was optimised by hand using daily summary statistics and the coefficient of efficiency for two objective functions. The basis for this multi-objective approach was introduced by Peel (1999).

The modelling objective was to achieve a percentage difference in mean, standard deviation and coefficient of variation between the observed and predicted daily streamflow of less than 1%. The coefficient of efficiency was also calculated from monthly data to provide insight into the quality of the model fit. The coefficient of efficiency was introduced by Nash & Sutcliffe (1970) and is shown in Equation 2.

$$Efficiency = \frac{\left(\sum_{i=1}^n (REC_i - \overline{REC})^2 - \sum_{i=1}^n (SIM_i - REC_i)^2 \right)}{\sum_{i=1}^n (REC_i - \overline{REC})^2} \times 100 \quad (2)$$

In Equation 2, REC_i is an observed monthly streamflow value, \overline{REC} is the observed average monthly streamflow and SIM_i is a simulated monthly streamflow. The first objective function used is the original Nash & Sutcliffe objective function shown in Equation 3.

$$OBJ1 = \sum_{i=1}^n (SIM_i - REC_i)^2 \quad (3)$$

Chiew et al. (1993) noted that high coefficient of efficiency values when using OBJ1 indicates that the model is reproducing large observed flows well. They also suggest that a second objective function derived from OBJ1, given in Equation 4, indicates whether the model is reproducing low observed flows well.

$$OBJ2 = \sum_{i=1}^n (SIM_i^{0.2} - REC_i^{0.2})^2 \quad (4)$$

Chiew et al. (1993) noted that simulations where the coefficient of efficiency = 0.6 are considered satisfactory and simulations where the coefficient of efficiency = 0.8 are considered acceptable. A coefficient of efficiency = 1.0 is a perfect reproduction of the observed data by the model. Through out the remainder of this report the value of the coefficient of efficiency when using objective function OBJ1 or OBJ2 will be referred to as simply OBJ1 or OBJ2 respectively for convenience.

Peel et al. (2000) noted that if the model was calibrated against OBJ1 and OBJ2 only, then the predicted streamflow had much less variability than the observed, which is an unsatisfactory result. Thus, the daily summary statistics are essential in order to guarantee that predicted streamflow has similar daily variability to the observed streamflow.

The calibration results for the North Esk catchment are presented in Table 4.1. The calibration period was 1/1/1950 – 31/12/1969.

Table 4.1
Calibration results for North Esk catchment.

| Catchment | Area (Ha) | SC | MC | Shape | Depth | Grad | Pscalar | OBJ1 | OBJ2 | % Mean | % StDev | % C _v |
|-----------|-----------|----|-------|-------|-------|-------|---------|-------|-------|--------|---------|------------------|
| North Esk | 36730 | 1 | 0.025 | 1 | 5 | 0.969 | 1.04 | 83.75 | 85.65 | -0.28 | -0.34 | -0.06 |

In Table 4.1, the parameters of Macaque used for calibration are:

- “SC” - the surface soil saturated hydraulic conductivity,
- “MC” - the minimum soil saturated hydraulic conductivity,
- “Shape” – a shape parameter expressing the rate of exponential decline in soil saturated hydraulic conductivity with depth,
- “Depth” – the depth at which minimum soil saturated hydraulic conductivity is reached,
- “Grad” the ratio of hydraulic to surface gradient,
- and “PScalar” which is the precipitation scaling parameter.

The precipitation scalar is multiplied by the incoming precipitation to produce the predicted precipitation at each ESU. The percentage difference between the observed and predicted daily streamflow means, standard deviations and coefficients of variation are represented in Table 4.1 by “% Mean”, “% StDev” and “% C_v” respectively.

It should be noted that although six parameters were available for calibration, only two were required to achieve the modelling objective. It was found that the precipitation scalar had a large influence over the predicted mean daily streamflow, while the ratio of the hydraulic to the surface gradient had a large influence over the variability of the predicted daily streamflow. The other parameters were set to default values that do not contradict the range of field-measured values.

Figure 4.1 shows predicted versus observed daily flow for the North Esk catchment from 1/1/1950 to 1/1/1954, which is part of the calibration period. The range of high and low flows appear to be well reproduced by Macaque over this period.

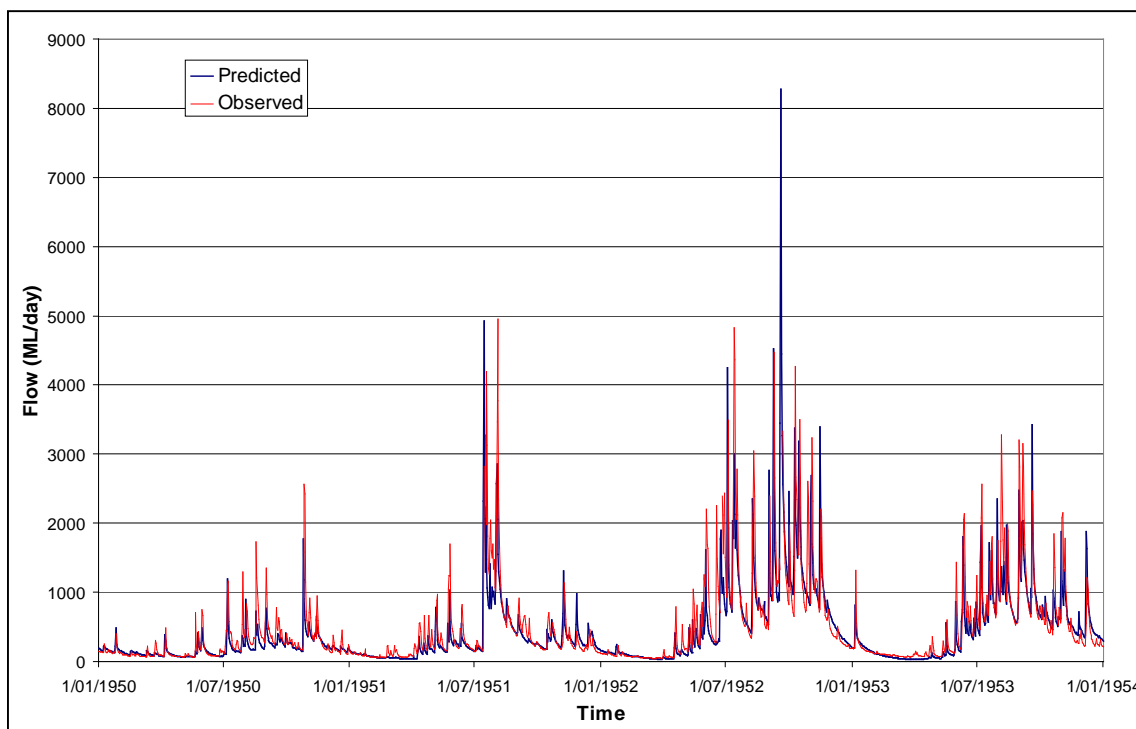


Figure 4.1 Calibrated predicted and observed daily flow for the North Esk @ The Ballroom catchment.

The calibrated values of OBJ1 and OBJ2 indicate that Macaque is modelling the North Esk catchment acceptably. A further test of how well Macaque performs is to look at the summary statistics and objective function values when the model is run on the non-calibration (verification) period of record (Table 4.2), which was from 1/1/1970 – 31/12/1998.

Table 4.2
Results for the North Esk for the verification period of record.

| Catchment | Area (Ha) | OBJ1 | OBJ2 | % Mean | % StDev | % C _v |
|-----------|-----------|-------|-------|--------|---------|------------------|
| North Esk | 36730 | 74.16 | 76.01 | -25.35 | -26.07 | -0.97 |

It can be seen from Table 4.2 that the model performance is worse for the verification period of record. In particular the daily mean and standard deviation are predicted to be 25% less than the observed. However, the predicted daily C_v is within 1% of the observed, which has resulted in the OBJ1 and OBJ2 values being satisfactory.

Figure 4.2 shows predicted versus observed daily flow for the North Esk catchment from 1/1/1995 to 31/12/1998, which is part of the verification period. High and low flows are not reproduced as well by Macaque over this period as in the calibration period.

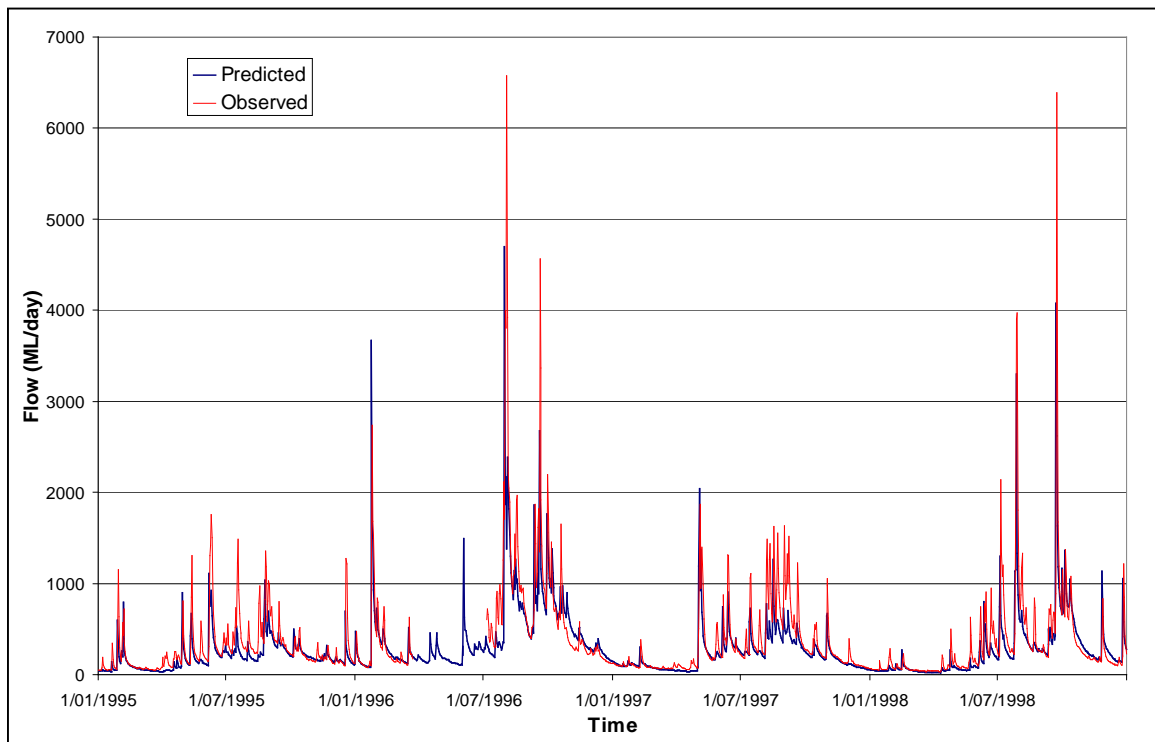


Figure 4.2 Verification predicted and observed daily flow for the North Esk @ The Ballroom catchment.

An analysis of daily mean precipitation, modelled and observed runoff for the calibration and verification periods (Table 4.3) reveals that the mean daily precipitation was 12% less in the verification period than the calibration period. The calibrated Macaque predicts mean daily runoff of 28% less in the verification period than the calibration period. The observed mean daily runoff is only 4% less between verification and calibration periods. An observed reduction in mean daily runoff of only 4% when mean daily precipitation is reduced by 12% over the same period is unusual and may indicate unrecorded changes to catchment vegetation type or age that were not modelled.

Table 4.3

Mean daily precipitation, modelled and observed runoff for the calibration and verification periods.

| Variable | Period | Mean (mm) |
|----------------------------|--------------|-----------|
| Mean Daily Precipitation | Calibration | 3.60 |
| | Verification | 3.15 |
| | % Diff | -12% |
| Modelled Mean Daily Runoff | Calibration | 1.29 |
| | Verification | 0.93 |
| | % Diff | -28% |
| Observed Mean Daily Runoff | Calibration | 1.30 |
| | Verification | 1.24 |
| | % Diff | -4% |

4.3 Flow Duration Curves

The previous section outlined the objective measures used to assess whether the model was successfully calibrated. Since the model results are to be used to investigate low flow conditions in the North Esk River, the quality of the models replication of the observed flow duration curve is assessed in this section.

The method of Vogel and Fennessey (1994) is used in order to objectively assess whether the modelled flow duration curves are statistically similar to the observed flow duration curve. Vogel and Fennessey (1994) noted that a method for estimating confidence intervals for a whole of record flow duration curve does not presently exist. They instead recommend constructing a series of daily flow duration curves for each complete year of record and then estimating confidence intervals for each quantile of the median annual flow duration curve. The steps involved in the methodology of Vogel and Fennessey (1994) are summarised below.

1. Sort the observed daily flow series into N complete years.
2. Rank each year of n observations of runoff q_i , where $i = 1, \dots, n$ in descending order, so that $q_{(1)}$ is the largest and $q_{(n)}$ is the smallest observation.
3. Add an extra observation $q_{(n+1)} = 0$ to each years record.
4. Use a quantile estimator to estimate the runoff Q_p for a given exceedance probability (p).
 - a. Vogel and Fennessey (1994) recommended several quantile estimators as suitable; the estimator used in this report is that of Parrish (1990) defined as $Q_p = (1 - \theta)q_{(i)} + \theta q_{(i+1)}$, where i is the integer component of $[np]$ and $\theta = [(n + 1)p - i + 0.5]$.
5. Quantiles are estimated for each year for a range of (p) values using the quantile estimator.
6. The N years of runoff data yield N estimates of $Q_p(i)$ for $i = 1, \dots, N$. The N values of $Q_p(i)$ are treated as a random sample from which confidence intervals $100(1 - \alpha)\%$ around the true quantile Q_p can be estimated.
7. To obtain upper ($Q_p(U)$) and lower ($Q_p(L)$) confidence intervals for Q_p the same quantile estimator is applied to the N values of $Q_p(i)$.
8. Steps 2 to 5 are repeated for each Q_p .
9. $Q_p(U)$ and $Q_p(L)$ for each Q_p are estimated from the quantile estimates from Step 8.
 - a. $Q_p(U) = (1 - \theta)Q_p(i) + \theta Q_p(i + 1)$, where i is the integer component of $[N(1 - \alpha/2)]$ and $\theta = N(1 - \alpha/2) - i + 0.5$ and α is the degree of confidence.
 - b. $Q_p(L) = (1 - \theta)Q_p(i) + \theta Q_p(i + 1)$, where i is the integer component of $[N(\alpha/2)]$ and $\theta = N(\alpha/2) - i + 0.5$ and α is the degree of confidence.

The methodology was applied to the observed runoff data for the calibration and verification periods. In the calibration period only 8 complete years were available, which were not enough for a meaningful analysis. Since the difference in observed mean daily runoff between calibration and verification periods is small (Table 4.3), the methodology was applied to the combined calibration and verification period.

The observed (1/1/1950 – 31/12/1998) and modelled runoff for the calibration period (1/1/1950 – 31/12/1969) median annual flow duration curves, with 90% confidence intervals are presented in Figure 4.3. The observed (1/1/1950 – 31/12/1998) and modelled runoff for the verification period (1/1/1970 – 31/12/1998) median annual flow duration curves, with 90% confidence intervals are presented in Figure 4.4. All flow duration curve data is presented in table form in Appendix A.

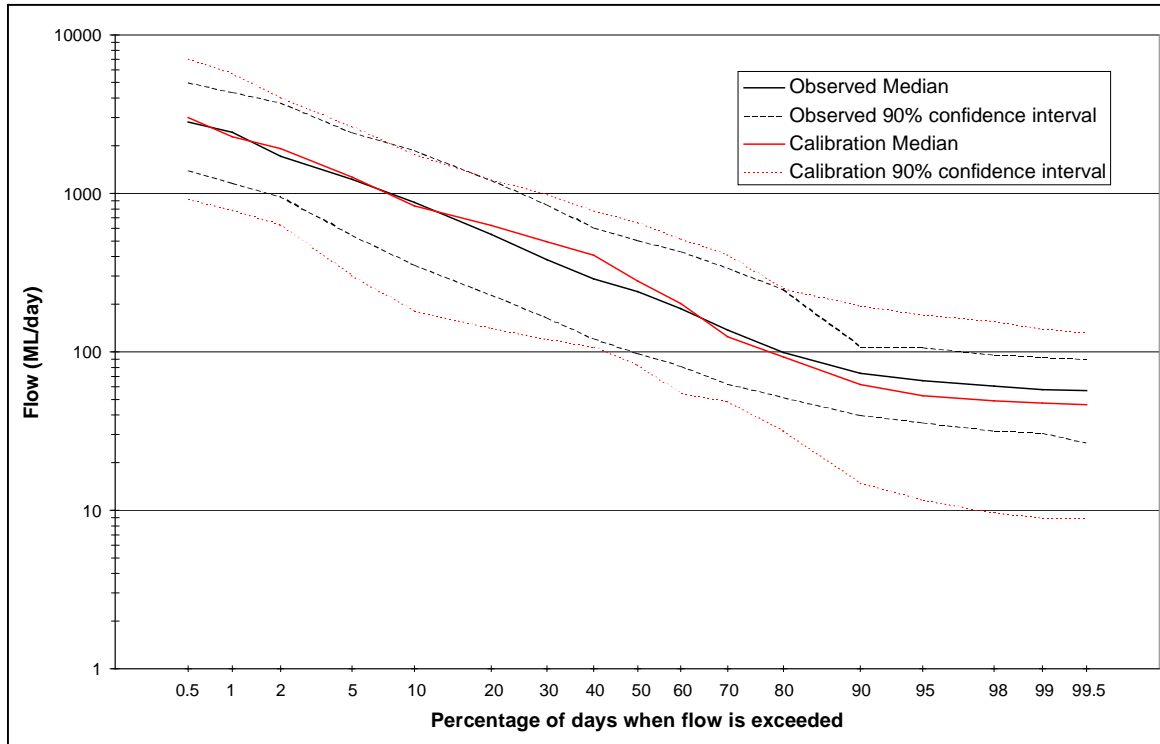


Figure 4.3 Observed (1/1/1950 – 31/12/1998) and modelled runoff for the calibration period (1/1/1950 – 31/12/1969) median annual flow duration curves, with 90% confidence intervals.

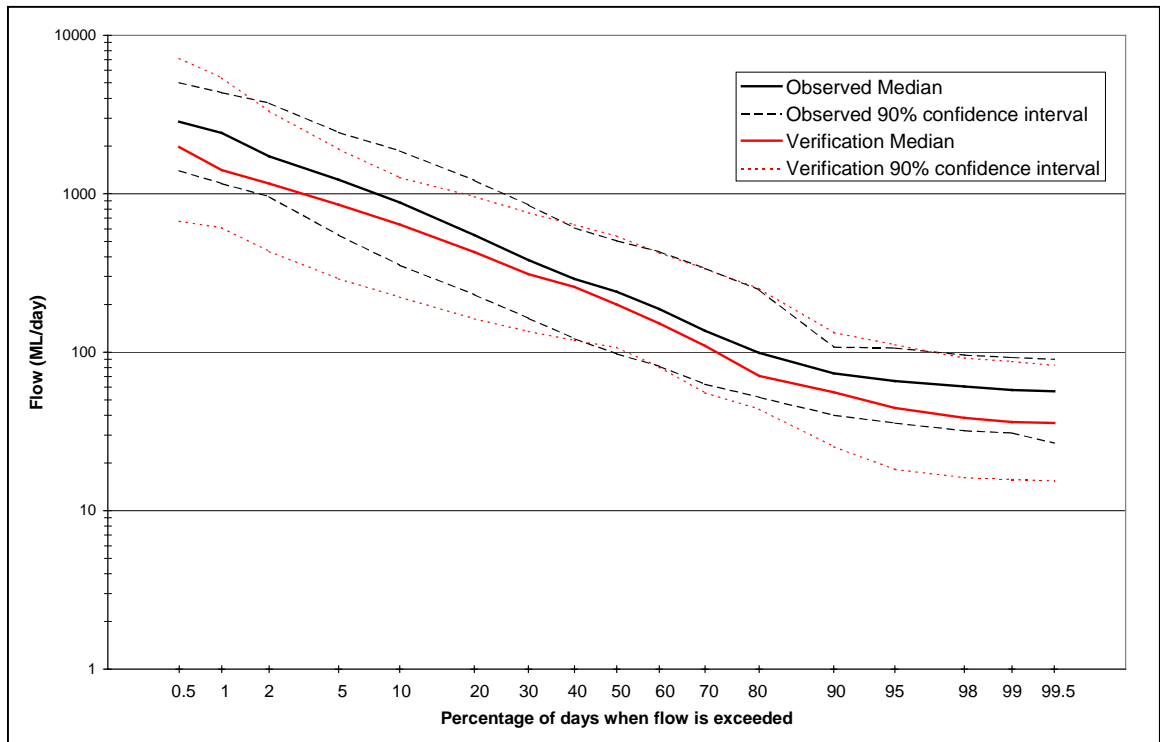


Figure 4.4 Observed (1/1/1950 – 31/12/1998) and modelled runoff for the verification period (1/1/1970 – 31/12/1998) median annual flow duration curves, with 90% confidence intervals.

The observed flow duration curves of Figures 4.3 and 4.4 are based on 33 complete years of runoff data. The modelled calibration flow duration curves of Figure 4.3 are based on 20 complete years and the modelled verification flow duration curves of Figure 4.4 are based on 29 complete years. The calibration 90% confidence interval is wider than the observed or verification confidence intervals, which is expected since the calibration confidence interval is based on one third less complete years.

The modelled runoff flow duration curves have a very similar shape to that of the observed runoff flow duration curve in Figures 4.3 and 4.4. This indicates that Macaque is modelling the rainfall / runoff processes in the catchment very well. In Figure 4.4 where the verification mean daily runoff is 25% less than the observed (see Table 4.2), the reduction in runoff is spread fairly evenly throughout the flow duration curve, with most reduction occurring in the high and low flow ends of the curve.

In Figure 4.3 the modelled low flows are slightly under estimated compared to the observed flows (on average 12% less for the lowest 40% of flows). In Figure 4.4 the lowest 40% of modelled flows are on average 29% less than the observed flows, when the average percentage difference is 27% across all flows.

4.4 Conclusions

The Macaque model was applied to the North Esk catchment. The quality of the calibration was acceptable and the verification was satisfactory. The shape of the modelled annual flow duration curves are similar to the observed flow duration curves for both the calibration and verification periods.

The spatial differences in modelled LAI compared to remotely sensed LAI indicates the potential for improvement in model performance if observed LAI data were available and if the vegetation type and vegetation age data was more accurate.

5. Predicting water yield impacts of logging rotation scenarios in the North Esk catchment

5.1 Introduction

The previous sections of this report described the Macaque model and demonstrated that it could be applied successfully to the North Esk catchment. In this section, the model is used to simulate the water yield impacts of different forest logging rotations and a catchment wide fire in the North Esk catchment. Firstly, the data requirements and methodology are outlined, followed by the results of the different forest logging scenarios.

5.2 Data and Methodology

Watson (1999) noted that in order to observe the impact of vegetation on water yield over a long period, the effects of climate variability have to be removed first. In this project the impact of changes in vegetation age and type will be investigated. A synthetic climate, with no interannual variability, was created and used as input to the Macaque model. The synthetic climate was created by taking the daily precipitation and temperature series of an average year, and repeating it for the number of years required. The year 1962 was chosen since its annual total precipitation and mean temperature were closest to the long-term means.

The synthetic climate was used in Macaque to assess the impact on water yield of four different logging rotation scenarios and a catchment wide fire. The four logging rotation scenarios are outlined below.

- 1) The E. regnans forest is logged and replanted at the rate of 1% of forested area per year (a 100 year rotation).
- 2) The E. regnans forest is logged and replanted at the rate of 2% of forested area per year (a 50 year rotation).
- 3) The E. regnans forest is logged and replanted at the rate of 5% of forested area per year (a 20 year rotation).
- 4) The E. regnans forest is logged and replanted at the rate of 5% of forested area per year (a 20 year rotation) and the pasture is converted to tree farms, logged and replanted at a rate of 5% of the tree farmed area per year (a 20 year rotation).

The selection of areas for logging each year was not random. Macaque uses a file called a "Unit" to store information about each ESU. The selection of areas for logging was determined by the order of ESU's in the Unit file. The area of all the ESU's covered by the vegetation type to be logged is the total area to be logged over one rotation. The area logged each year was the total area to be logged multiplied by the rotation rate. The ESU's that will be logged in the first year were found by searching through the Unit file for ESU's covered in the appropriate vegetation type that had a combined ESU area equal to the area to be logged each year. Once enough ESU's had been found for that year, they were marked as having been logged and could not be logged again in that rotation. Each year's logged area was determined by this method.

Each logging scenario was run for 2 rotations. In the first rotation, pre-existing (often mature) forest or pasture is replaced by E. regnans (in the case of forest) or E. nitens (in the case of tree farming). In the second rotation the regrowth is logged and replanted. The first rotation models the water yield impact of the introduction of a logging rotation policy, while the second rotation models the long-term water yield impact once a logging rotation is established.

Comparison of the simulation and observed daily summary statistics and flow duration curves will be used to assess the impact on water yield of the logging rotations and the catchment wide fire. The observed daily summary statistics and flow duration curve are based on observed data from 1/1/1950 – 31/12/1998.

Macaque requires real dates in order to run, so the simulations were conducted in the future. All scenario simulations started on the 1/1/2010, which is an arbitrarily chosen date. The catchment vegetation type and age are assumed to be undisturbed from the present until the 1/1/2010.

When a leap year is modelled using the synthetic climate, values for the 29/2 are required to be added to the time series of precipitation and temperature. The annual daily average precipitation is used for precipitation and February maximum and minimum averages are used for temperature.

A potential future analysis would be to assess the impact on water yield of the logging rotation and catchment wide fire scenarios under a stochastically generated synthetic climate that is statistically similar to the observed climate. This analysis would assess the impact on water yield of the logging rotations and catchment wide fire due to both the changing vegetation and the climate variability.

5.3 Simulation results

The simulated and observed daily summary statistics of the first scenario (100 year rotation) are presented in Table 5.1. Compared to the observed runoff a reduction in the mean daily flow of 5% occurs over the first rotation and a reduction in the mean daily flow of 15% occurs over the second rotation. In both rotations the variability of the daily runoff is reduced by about 15%.

Table 5.1

Simulated and observed daily runoff summary statistics for the first logging scenario (100 year rotation).

| Variable | Period | Mean (ML) | StDev (ML) | Cv |
|----------------------------------|-----------------------|-----------|------------|------|
| Observed Daily Runoff | 1/1/1950 – 31/12/1998 | 465 | 610 | 1.31 |
| 1 st Rotation | 1/1/2010 – 31/12/2108 | 440 | 484 | 1.10 |
| 2 nd Rotation | 1/1/2109 – 31/12/2207 | 393 | 439 | 1.12 |
| % Diff Obs. 1 st Rot. | | -5% | -21% | -16% |
| % Diff Obs. 2 nd Rot. | | -15% | -28% | -15% |

The median flow duration curves and 90% confidence intervals of the simulated and observed runoff are presented in Figure 5.1. The width of the confidence intervals is greatly reduced for the first and second rotation flow duration curves due to there being no climate variability modelled in the simulations and also the larger sample size (98 years). The first rotation flow duration curves are similar to the observed median curve with the observed median curve within the simulated 90% confidence interval for most of the range of probabilities of exceedance, in particular the low flow end. The second rotation flow duration curves are also similar to the observed median curve although the observed median curve is not within the simulated 90% confidence interval for most of the range of probabilities of exceedance, in particular the low flow end. The second rotation simulated low flows are generally 15% below the observed for the lowest 40% of flows.

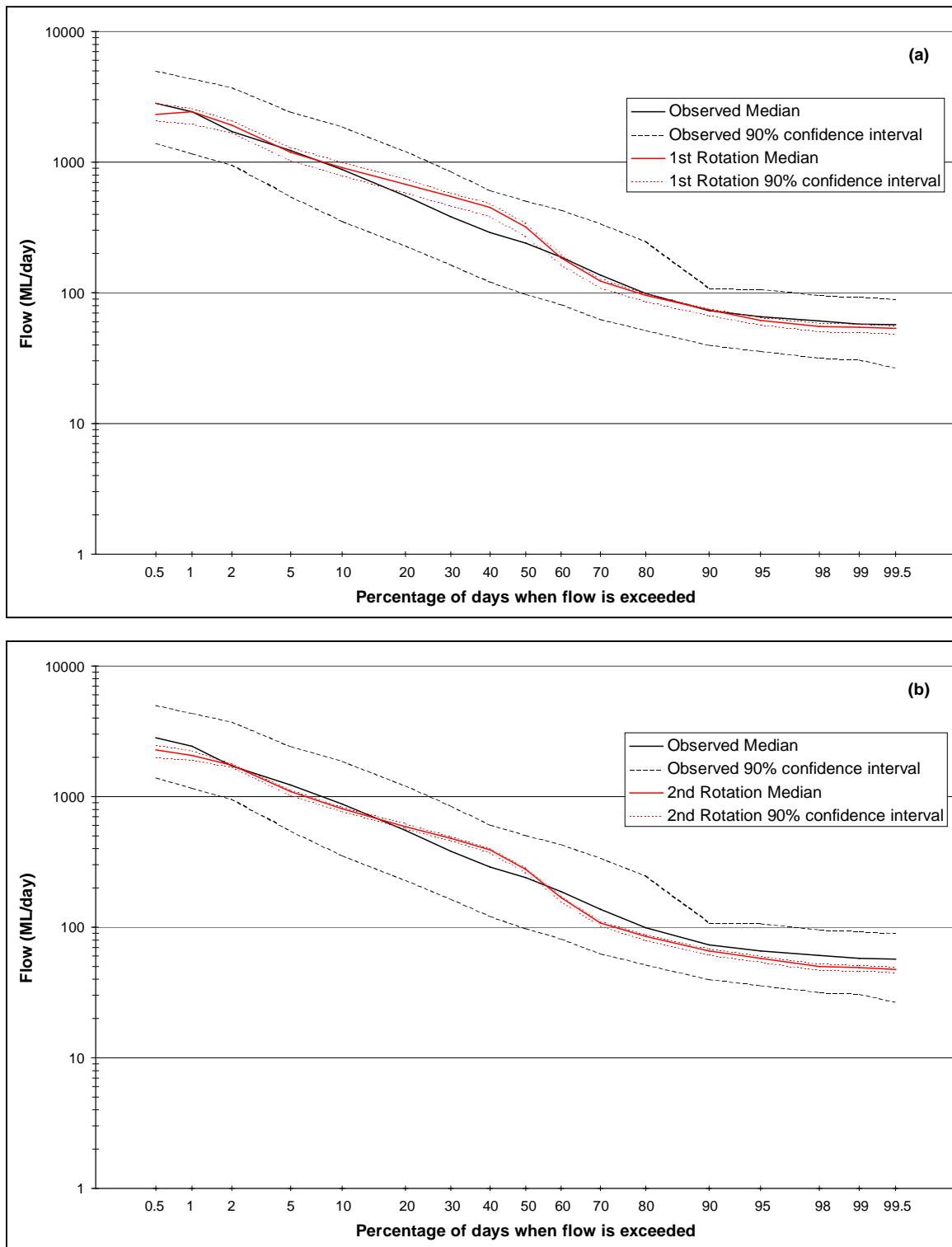


Figure 5.1 Observed and modelled median annual flow duration curves, with 90% confidence intervals for the 1st rotation (a) and second rotation (b) of the 100-year rotation.

Both Table 5.1 and Figure 5.1 indicate that the impact of a 100-year logging rotation scenario in terms of water yield on the North Esk catchment is small. The first rotation low flows are not discernibly different from the observed low flows, while the second rotation low flows are generally 15% lower than the observed low flows. Considering that the lowest 40% of flows were 12% lower than the observed in the calibration, there is very little difference in low flows between the second rotation and the calibration.

The simulated and observed daily summary statistics of the second scenario (50 year rotation) are presented in Table 5.2. Compared to the observed runoff a reduction in the mean daily flow of 6% occurs

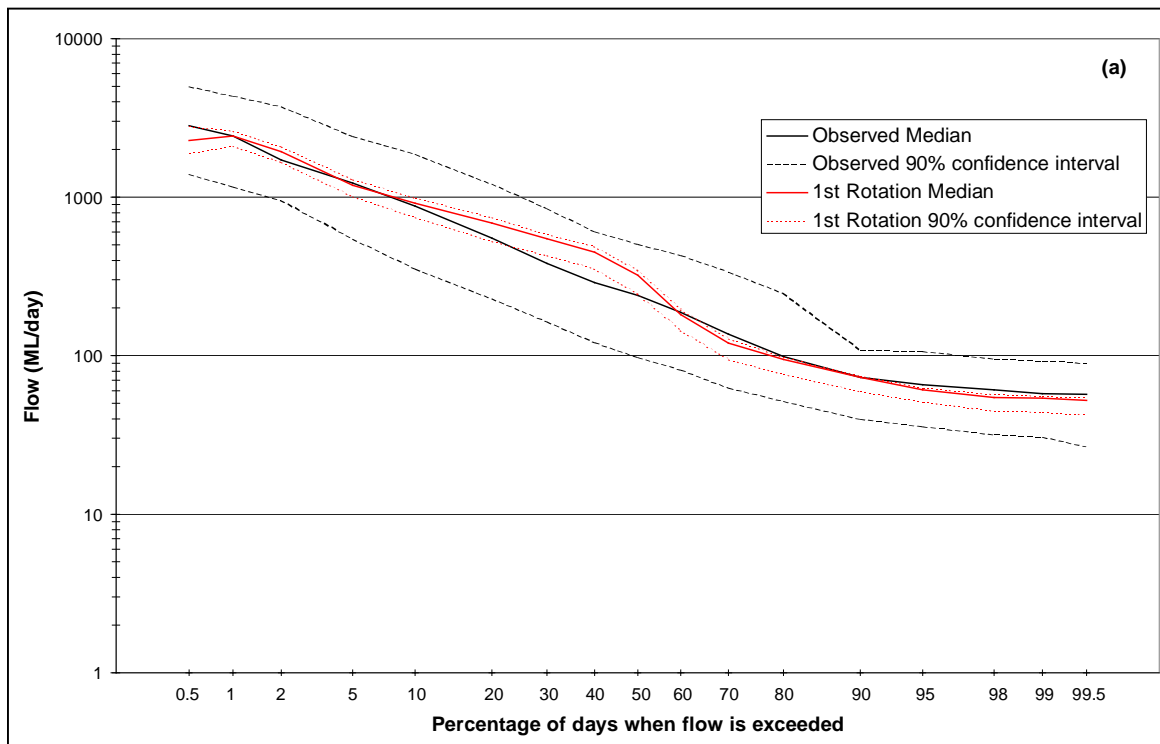
over the first rotation and a reduction in the mean daily flow of 21% occurs over the second rotation. In both rotations the variability of the daily runoff is reduced by about 15%.

Table 5.2

Simulated and observed daily runoff summary statistics for the second logging scenario (50 year rotation).

| Variable | Period | Mean (ML) | StDev (ML) | Cv |
|----------------------------------|-----------------------|-----------|------------|------|
| Observed Daily Runoff | 1/1/1950 – 31/12/1998 | 465 | 610 | 1.31 |
| 1 st Rotation | 1/1/2010 – 31/12/2060 | 436 | 489 | 1.12 |
| 2 nd Rotation | 1/1/2061 – 31/12/2111 | 368 | 416 | 1.13 |
| % Diff Obs. 1 st Rot. | | -6% | -20% | -15% |
| % Diff Obs. 2 nd Rot. | | -21% | -32% | -14% |

The median flow duration curves and 90% confidence intervals of the simulated and observed runoff are presented in Figure 5.2. The first rotation flow duration curves are similar to the observed median curve with the observed median curve within the simulated 90% confidence interval for some of the range of probabilities of exceedance. The low flow end of the simulated curves is just below the observed median curve. The second rotation flow duration curves also have a similar shape to the observed median curve although the observed median curve is not within the simulated 90% confidence interval for most of the range of probabilities of exceedance, in particular the low flow end. The second rotation simulated low flows are generally 20% below the observed for the lowest 40% of flows.



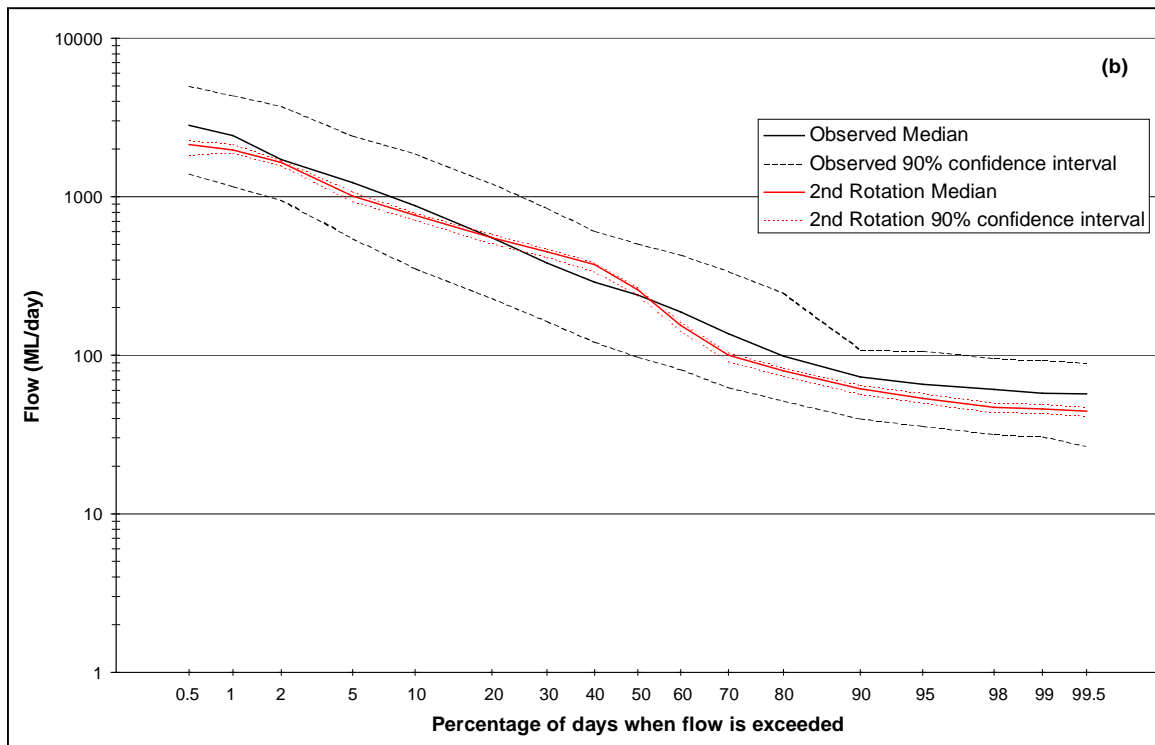


Figure 5.2 Observed and modelled median annual flow duration curves, with 90% confidence intervals for the 1st rotation (a) and second rotation (b) of the 50-year rotation.

Both Table 5.2 and Figure 5.2 indicate that the impact of a 50-year logging rotation scenario in terms of water yield on the North Esk catchment is increased compared to the impact of the 100-year rotation. The first rotation low flows are slightly less than the observed low flows, while the second rotation low flows are generally 20% lower than the observed low flows. Considering that the lowest 40% of flows were 12% lower than the observed in the calibration, the second rotation low flows are slightly lower than the calibrated runoff.

The simulated and observed daily summary statistics of the third scenario (20 year rotation) are presented in Table 5.3. Compared to the observed runoff a reduction in the mean daily flow of 3% occurs over the first rotation and a reduction in the mean daily flow of 20% occurs over the second rotation. In both rotations the variability of the daily runoff is reduced by about 15%.

Table 5.3

Simulated and observed daily runoff summary statistics for the third logging scenario (20 year rotation).

| Variable | Period | Mean (ML) | StDev (ML) | Cv |
|----------------------------------|-----------------------|-----------|------------|------|
| Observed Daily Runoff | 1/1/1950 – 31/12/1998 | 465 | 610 | 1.31 |
| 1 st Rotation | 1/1/2010 – 31/12/2030 | 451 | 500 | 1.11 |
| 2 nd Rotation | 1/1/2031 – 31/12/2051 | 370 | 419 | 1.13 |
| % Diff Obs. 1 st Rot. | | -3% | -18% | -16% |
| % Diff Obs. 2 nd Rot. | | -20% | -31% | -14% |

The median flow duration curves and 90% confidence intervals of the simulated and observed runoff are presented in Figure 5.3. The first rotation flow duration curves are similar to the observed median curve with the observed median curve within the simulated 90% confidence interval for most of the range of probabilities of exceedance, in particular the low flow end. The second rotation flow duration curves also have a similar shape to the observed median curve although the observed median curve is not within the simulated 90% confidence interval for most of the range of probabilities of exceedance, in particular the low flow end. The second rotation simulated low flows are generally 21% below the observed for the lowest 40% of flows.

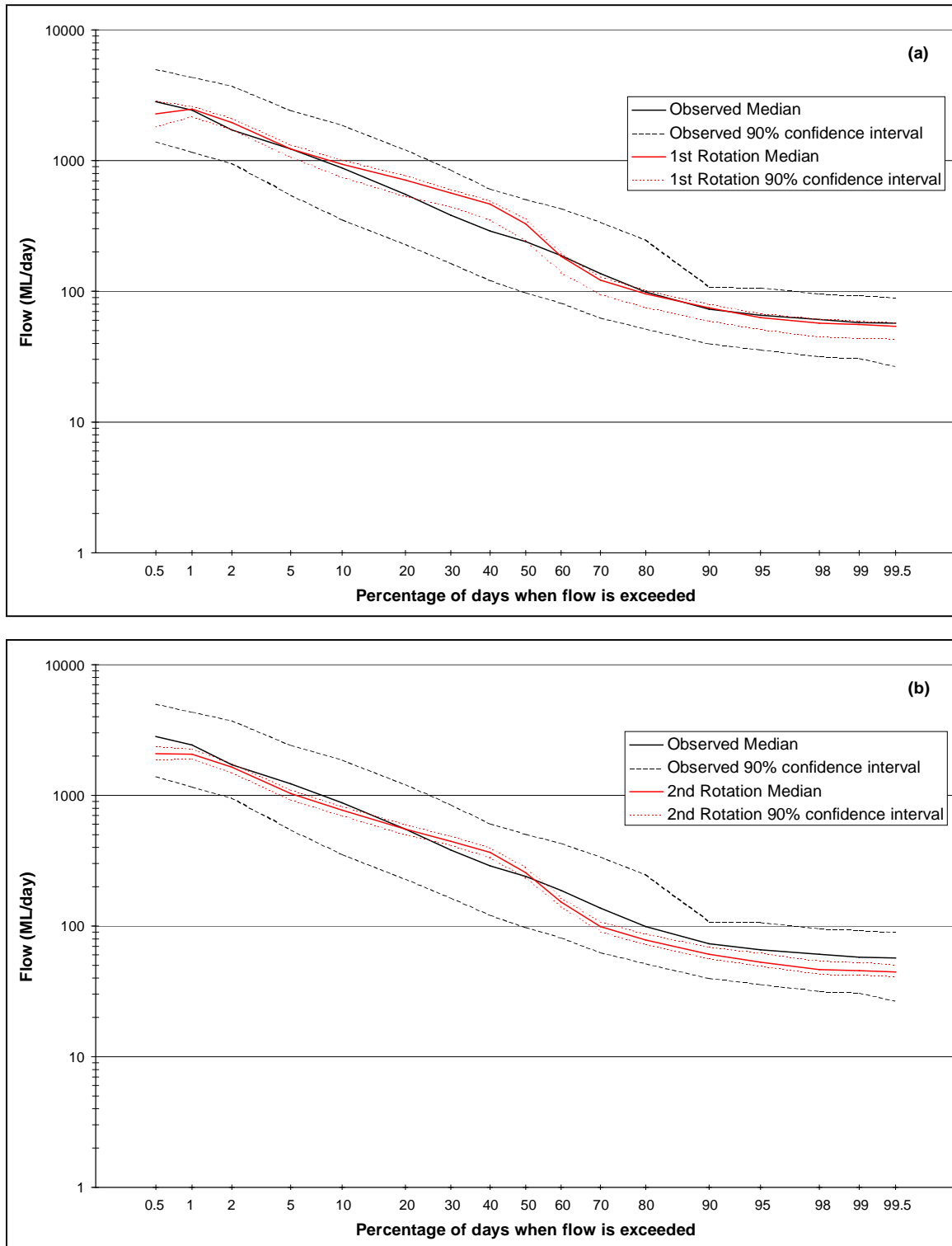


Figure 5.3 Observed and modelled median annual flow duration curves, with 90% confidence intervals for the 1st rotation (a) and second rotation (b) of the 20-year rotation.

Both Table 5.3 and Figure 5.3 indicate that the impact of a 20-year logging rotation scenario in terms of water yield on the North Esk catchment is similar to the impact of the 50-year rotation. The first rotation low flows are slightly less than the observed low flows, while the second rotation low flows are generally 20% lower than the observed low flows. Considering that the lowest 40% of flows were 12% lower than the observed in the calibration, the second rotation low flows are slightly lower than the calibrated runoff.

The simulated and observed daily summary statistics of the fourth scenario (20 year rotation of forest and tree farm) are presented in Table 5.4. Compared to the observed runoff a reduction in the mean daily

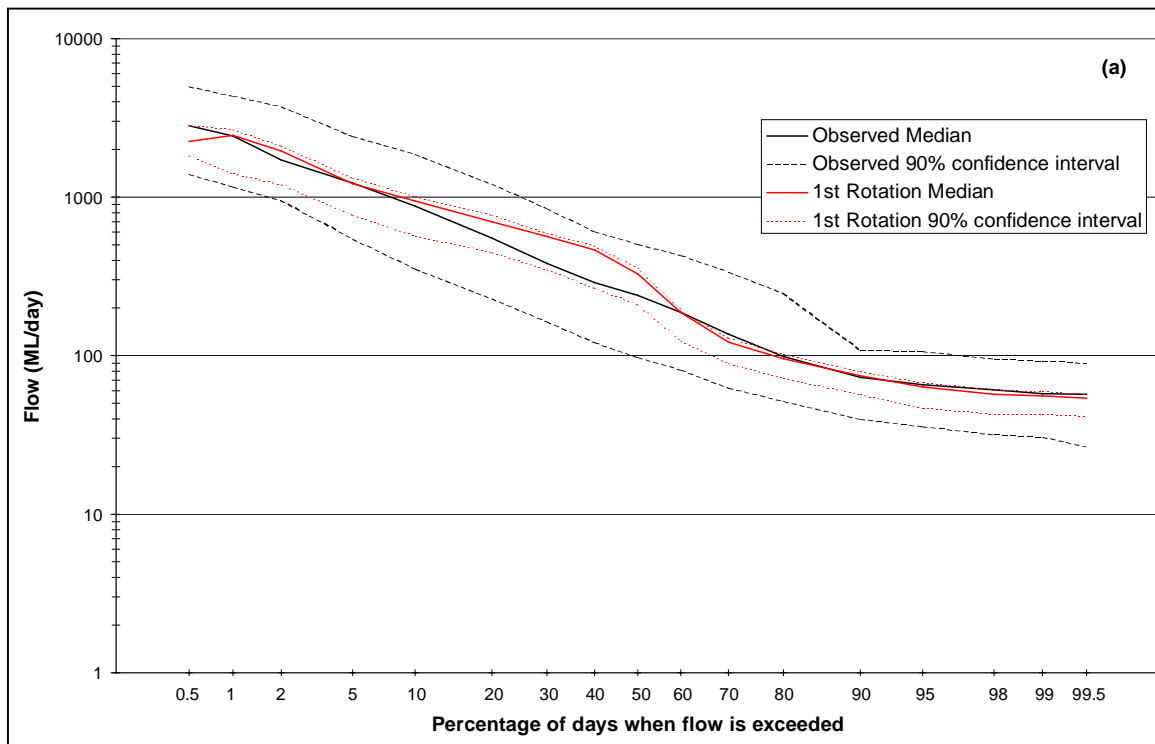
flow of 4% occurs over the first rotation and a reduction in the mean daily flow of 33% occurs over the second rotation. In the first rotation the variability of the daily runoff is reduced by about 15% and by 23% in the second rotation.

Table 5.4

Simulated and observed daily runoff summary statistics for the fourth logging scenario (20 year rotation of forest and tree farm).

| Variable | Period | Mean (ML) | StDev (ML) | Cv |
|----------------------------------|-----------------------|-----------|------------|------|
| Observed Daily Runoff | 1/1/1950 – 31/12/1998 | 465 | 610 | 1.31 |
| 1 st Rotation | 1/1/2010 – 31/12/2030 | 448 | 498 | 1.11 |
| 2 nd Rotation | 1/1/2031 – 31/12/2051 | 310 | 313 | 1.01 |
| % Diff Obs. 1 st Rot. | | -4% | -18% | -15% |
| % Diff Obs. 2 nd Rot. | | -33% | -49% | -23% |

The median flow duration curves and 90% confidence intervals of the simulated and observed runoff are presented in Figure 5.4. The first rotation flow duration curves are similar to the observed median curve with the observed median curve within the simulated 90% confidence interval for most of the range of probabilities of exceedance, in particular the low flow end. The second rotation flow duration curves are generally below the observed median curve with the observed median curve within the simulated 90% confidence interval for a small range of probabilities of exceedance. The simulated low flows are well below the observed low flows. The second rotation simulated low flows are generally 25% below the observed for the lowest 40% of flows.



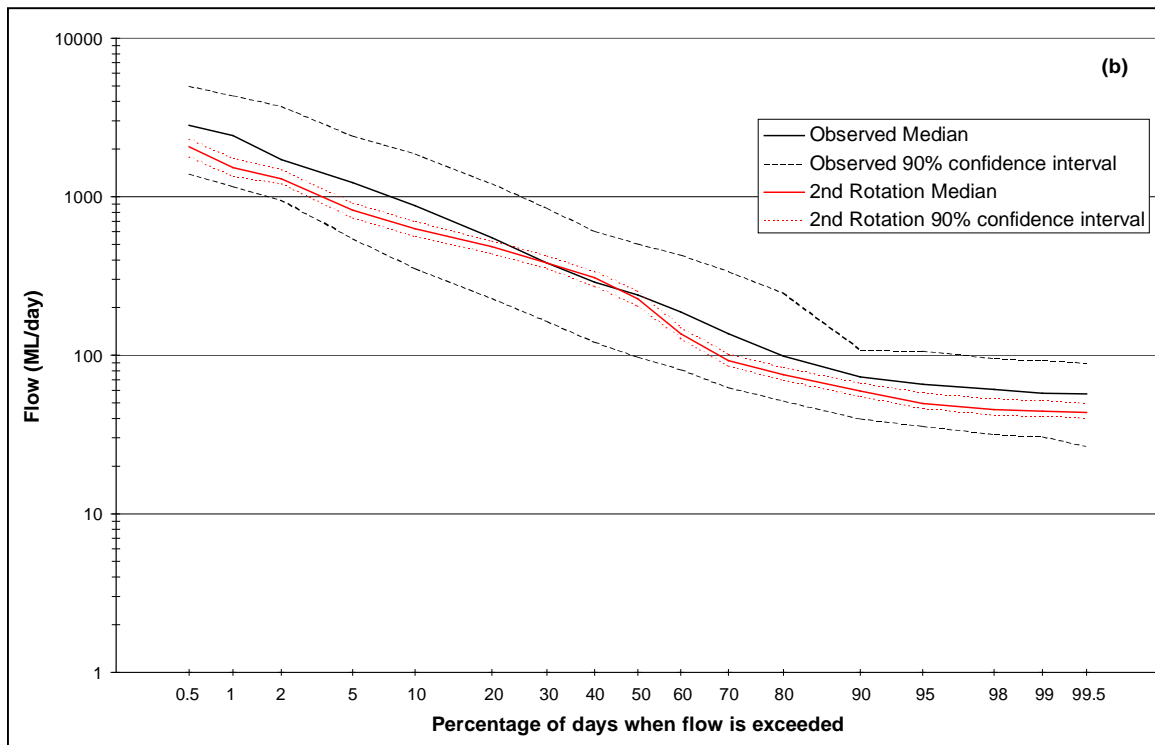


Figure 5.4 Observed and modelled median annual flow duration curves, with 90% confidence intervals for the 1st rotation (a) and second rotation (b) of the 20-year rotation for forest and tree farm.

Both Table 5.4 and Figure 5.4 indicate that the impact of a 20-year logging of forest and tree farm rotation scenario in terms of water yield on the North Esk catchment has the greatest impact of the logging rotation scenarios. In the first rotation low flows are similar to the observed low flows, while the second rotation low flows are generally 25% lower than the observed low flows. Considering that the lowest 40% of flows were 12% lower than the observed in the calibration, the second rotation low flows are significantly lower than the calibrated runoff.

The simulated maximum impact and observed daily summary statistics of the catchment wide fire scenario are presented in Table 5.5. The maximum impact was found to occur in 2018, which is eight years after the fire. Compared to the observed runoff the maximum impact on water yield is a reduction in the mean daily flow of 44%. The variability of the daily runoff in 2018 is 5% lower than the variability of the observed daily runoff.

Table 5.5

Simulated maximum impact and observed daily runoff summary statistics for the catchment wide fire scenario.

| Variable | Period | Mean (ML) | StDev (ML) | Cv |
|-----------------------|-----------------------|-----------|------------|------|
| Observed Daily Runoff | 1/1/1950 – 31/12/1998 | 465 | 610 | 1.31 |
| 2018 | 1/1/2018 – 31/12/2018 | 260 | 325 | 1.25 |
| % Diff Obs. 2018. | | -44% | -47% | -5% |

The median flow duration curve and 90% confidence interval of the observed runoff and the flow duration curve of the simulated maximum impact year are presented in Figure 5.5. The simulated maximum impact flow duration curve is consistently below the median observed flow duration curve and is outside the observed 90% confidence interval for the lowest 30% of flows. The maximum impact simulated low flows are generally 50% below the observed for the lowest 40% of flows.

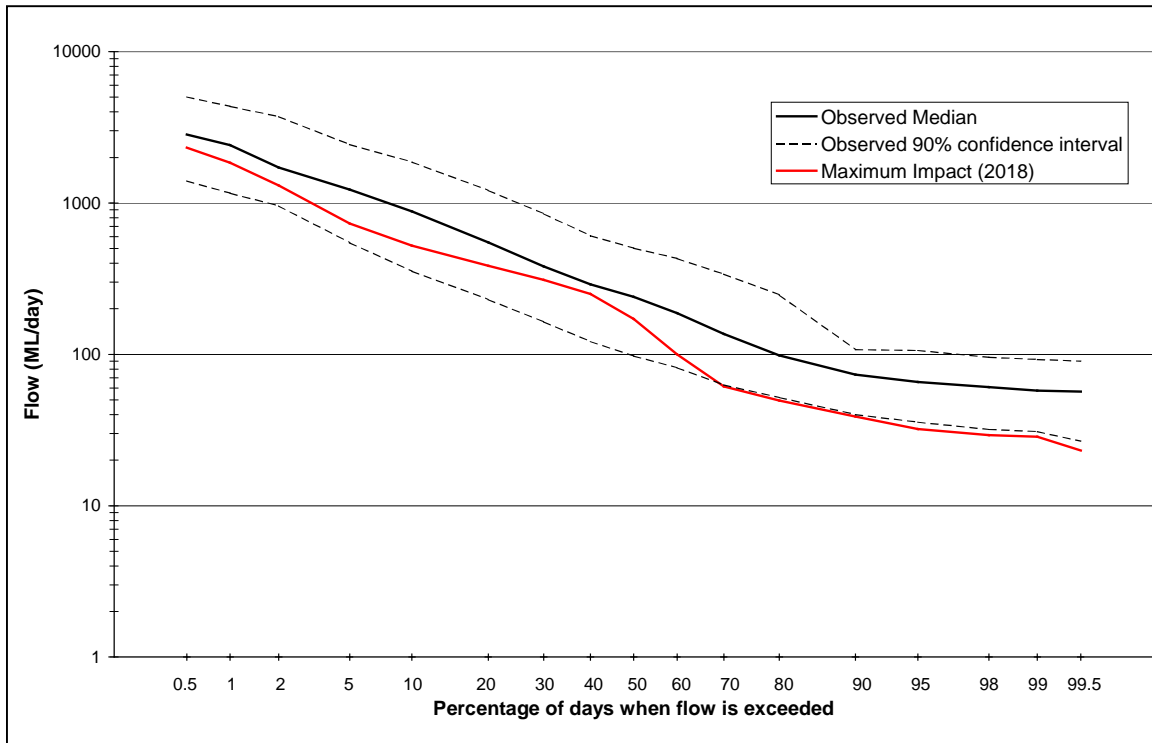


Figure 5.5 Observed median annual flow duration curve with 90% confidence interval and maximum impact flow duration curve for the year 2018.

Both Table 5.5 and Figure 5.5 indicate that the impact of a catchment wide fire scenario in terms of water yield on the North Esk catchment is very large. The maximum impact low flows are generally 50% lower than the observed low flows. Considering that the lowest 40% of flows were 12% lower than the observed in the calibration, there is very significant reduction in low flows between the maximum impact of a fire and the calibration.

A summary of the impact on mean daily flow and the lowest 40% of flows is provided in Table 5.6 for all the scenarios.

Table 5.6

Summary of the impact on mean daily flow and the lowest 40% of flows relative to the observed data for all scenarios.

| Scenario | Rotation | Mean Daily Flow (ML) | % Diff from Observed Mean Daily Flow | Average % Diff from Observed Lowest 40% of Flows |
|----------------------------|-----------------|----------------------|--------------------------------------|--|
| Observed (1950-1998) | | 465 | | |
| Calibration (1950-69) | | 480 | 3% | -12% |
| 100 Year Forest | 1 st | 440 | -5% | -5% |
| 100 Year Forest | 2 nd | 393 | -15% | -15% |
| 50 Year Forest | 1 st | 436 | -6% | -6% |
| 50 Year Forest | 2 nd | 368 | -21% | -20% |
| 20 Year Forest | 1 st | 451 | -3% | -4% |
| 20 Year Forest | 2 nd | 370 | -20% | -21% |
| 20 Year Forest & Tree Farm | 1 st | 448 | -4% | -4% |
| 20 Year Forest & Tree Farm | 2 nd | 310 | -33% | -25% |
| Catchment Wide Fire | | 260 | -44% | -50% |

5.4 Discussion

The main determinant of whether a logging rotation scenario will influence the total runoff and in particular low flows is the degree to which the area logged contributes to total runoff or low flows. In order to investigate which areas contribute to total runoff and low flows in a climatically average year the

calibrated Macaque was run for the year 1962. Table 5.7 presents the percentage of the catchment area covered by each vegetation type and the percentage of rainfall received and total runoff produced from that vegetation type. Although E. regnans covers 61.3% of the catchment area and receives 58.9% of the total precipitation only 36.9% of the total runoff is produced from that area. Grassland covers 11.8% of the catchment, receives 10.8% of the precipitation and produces 17.8% of the total runoff. Heath covers only 3.1% of the catchment area, receives 5.0% of the precipitation and produces 11.7% of the total runoff, while Rocky covers 1.7% of catchment area, receives 2.2% of the precipitation and produces 5.3% of the total runoff. The heath and rocky areas are mainly located on and around Ben Lomond, the highest and wettest part of the catchment. The E. regnans areas are generally in the lower and dryer parts of the catchment. In a climatically average year any logging rotation simulations that involve only E. regnans would potentially modify 36.9% of the total runoff, while a logging and tree farm rotation simulation potentially modifies 54.7% of the total runoff.

Table 5.7 also contains the percentage of precipitation received and runoff produced from each vegetation type for the three months with the lowest flow (January, February and March). The area covered by E. regnans receives 58.0% of the precipitation and produces 29.3% of the runoff for these three months, grassland receives 10.3% of the precipitation and produces 4.2% of the runoff, while heath and rocky areas receive 7.9% of the precipitation and produce 33.0% of the runoff. In a climatically average year any logging rotation simulations that involve only E. regnans would potentially modify 29.3% of the runoff in the driest three months, while a logging and tree farm rotation simulation potentially modifies 33.5% of the runoff in the driest three months.

Table 5.7

Percentage of catchment area covered by a particular vegetation type, precipitation received and runoff produced for annual and the driest three months of 1962 for the North Esk at the Ballroom.

| Vegetation Type | % of total Area | % of total Precipitation | % of total Runoff | % of driest 3 months Precipitation | % of driest 3 months Runoff |
|-------------------------|------------------------|---------------------------------|--------------------------|---|------------------------------------|
| E. regnans | 61.3% | 58.9% | 36.9% | 58.0% | 29.3% |
| Grassland | 11.8% | 10.8% | 17.8% | 10.3% | 4.2% |
| E. obliqua | 17.9% | 19.0% | 25.7% | 19.8% | 32.9% |
| Acacia dealbata | 1.6% | 1.5% | 1.0% | 1.5% | 0.3% |
| Nothofagus cunninghamii | 2.6% | 2.6% | 1.7% | 2.6% | 0.3% |
| Heath | 3.1% | 5.0% | 11.7% | 5.5% | 22.9% |
| Rocky | 1.7% | 2.2% | 5.3% | 2.4% | 10.1% |

The analysis presented in Table 5.7 indicates that 45.3% of the modelled total runoff and 66.5% of the modelled runoff in the driest three months of the climatically average year of 1962 will be unaffected by changes in vegetation age or type introduced by the logging rotations and tree farm scenarios.

The larger the proportion of total runoff and the driest three months runoff unaffected by the logging and tree farm scenarios the narrower the range of the potential impact of those scenarios. This is seen in the results of the flow duration curve analysis presented in the previous sub-section. The impact of the different scenarios on the lowest 40% of flows ranged between reductions of 15% to 25% for the second rotation. Considering that the areas modified in the scenarios contributed 33.5% of the runoff for the three driest months, reductions ranging from 15% to 25% represent significantly impacted runoff from the modified areas. The impact of the difference scenarios on mean daily runoff ranged between reductions of 15% to 33% for the second rotation. Considering that the areas modified in the scenarios contributed 54.7% of the total runoff, reductions ranging from 15% to 33% represent significantly impacted runoff from the modified areas, although the impact on low flows for the modified areas is greater than that for total runoff.

The modelled impact on low flows is smaller than the modelled impact on mean daily runoff due to the unmodified areas of the catchment contributing a larger proportion of runoff for low flows than for total runoff.

The greater impact on water yield of the 20-year rotations compared to the 100-year rotation is due to the resulting difference in average LAI of the modified forest. Over a 100-year rotation a forest of E. regnans has an average age of 50 years, which from Figure 3.5 results in an LAI that is close to 4.0. Figure 3.5

indicates that a mature forest (average age of 250 years) will have an LAI close to 3.5. The 20-year rotation produces a forest with an average age of 10, which from Figure 3.5 is near the maximum LAI (about 5.2) and the minimum water yield (Watson et al., 1999b). Appendix B contains a summary of annual evapotranspiration by species for the climatically average (1962) simulation and the 2nd rotation of the 20-year logging and tree-farming scenario.

The catchment wide fire scenario has the greatest impact on water yield since all the vegetation is burnt at the same time. The entire *E. regnans* forest is the same age and regenerates according to the LAI versus time curve shown in Figure 3.5. Eight years after the fire the *E. regnans* forest is at maximum LAI (Figure 3.5), minimum water yield (Watson et al., 1999b) and thus maximum impact on water yield.

5.5 Application to St Patricks catchment

The lack of good quality streamflow data for the St Patricks catchment precluded a modelling analysis, however, the insights derived from the North Esk modelling analysis make some comments about the St Patricks catchment possible.

The digital elevation model and vegetation type for the St Patricks catchment are shown in Figure 5.6. The importance of a region like Ben Lomond as a source area of total runoff and in particular low flows for the North Esk catchment was noted in the previous sub-section. In the St Patricks catchment the mountains are lower than Ben Lomond and do not have an extensive alpine plateau of heath. However, a large area of rock is located in the “Non Forest” area on Mt Barrow. In the North Esk 50.3% of the catchment was covered by “Eucalypt Tall Forest”, which was modelled as *E. regnans*. In the St Patricks catchment 39.0% of the catchment area is covered by “Eucalypt Tall Forest”. The area of grassland in the St Patricks catchment is also likely to be less than in the North Esk, once the “Non Forest” category of vegetation is divided into Heath, Rocky and Grassland. Thus the proportion of the St Patricks catchment that would be modified in a logging or tree farm simulation is less than that in the North Esk catchment. However, the proportion of unmodified runoff in the St Patricks catchment may be less than the North Esk, due to the likelihood of smaller areas of rocky and heath vegetation. It is expected that the total runoff and low flows of the St Patricks River would be impacted in a similar way as those in the North Esk if the same logging rotation, tree farm and catchment wide fire scenarios were applied to the catchment.

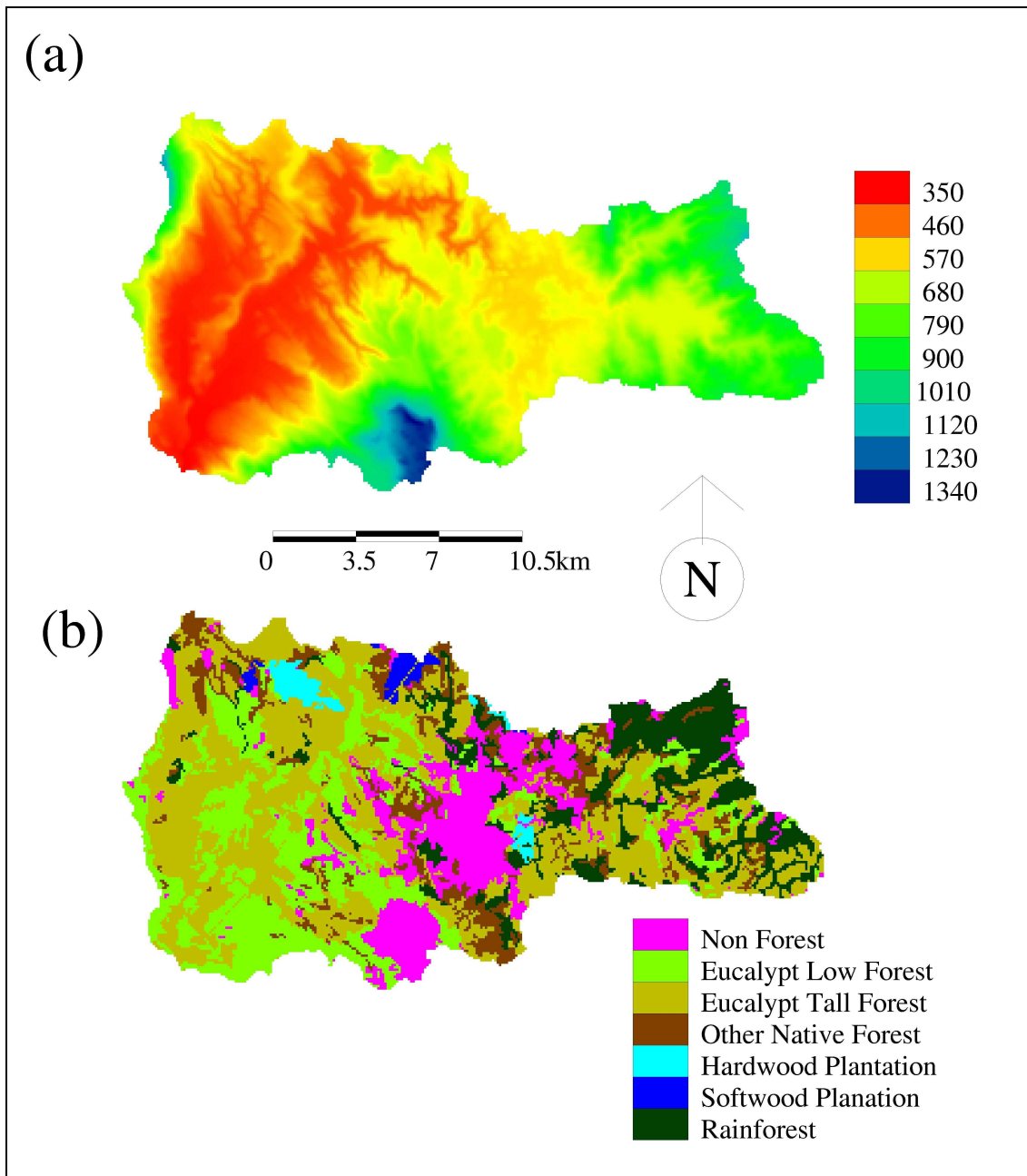


Figure 5.6 St Patricks catchment (a) digital elevation model (in metres) and (b) vegetation type.

5.6 Conclusion

Daily climate data from 1962 was used to create a synthetic climate with no interannual variability for use in the scenario modelling. Four logging rotation and tree farm scenarios were modelled with Macaque for the North Esk catchment using a synthetic climate. Total runoff and low flows were affected least in the 100-year logging rotation scenario and most in the 20-year logging rotation and tree farm scenario. The range of mean daily flow impact of the scenarios was a reduction of 3% for the first rotation of the 20-year logging rotation to a 33% reduction for the second rotation of the 20-year logging rotation and tree farm scenario. The range of impact on the lowest 40% of flows was a 4% reduction for the first rotation of the 20-year logging rotation scenario to a 25% reduction for the 20-year logging rotation and tree farm scenario. Considering that the lowest 40% of flows were 12% lower than the observed in the calibration, the 20-year logging rotation and tree farm scenario second rotation low flows are significantly lower than the calibrated runoff.

A catchment wide fire scenario was also modelled using the synthetic climate. The maximum impact on water yield occurred eight years after the fire. The maximum impact of the fire scenario on mean daily flow was a reduction of 44% and the lowest 40% of flows were reduced by 50% relative to the observed data.

The year 1962 was also modelled in order to investigate the source areas of modelled total runoff and low flows in a climatically average year. Areas covered in E. regnans and grassland account for 73% of the catchment area and produce 54.7% of the total runoff and 33.5% of the runoff for the three driest months (low flows). The modelled impact of the logging rotation scenarios on low flows is smaller than the modelled impact on mean daily runoff due to the modified areas of the catchment contributing a smaller proportion of runoff for low flows than for total runoff.

The impact on water yield of the 20-year rotations is greater than that of the 100-year rotation, due to the difference in resultant average forest age, LAI and water yield. The 20-year rotation forest (average age of 10) has higher values of LAI and thus lower water yield than the 100-year rotation forest (average age of 50).

The potential impact on total runoff and low flows of the same logging rotation, tree farm and fire scenarios on the St Patricks catchment is likely to be similar to that modelled in the North Esk since the St Patricks catchment has a smaller area of E. regnans and grassland, but also a smaller area of heath and rock.

6. Predicting water yield impacts of logging rotation scenarios in the North Esk catchment under a variable climate

6.1 Introduction

The previous section of this report described the application of Macaque to predict the effect of logging rotations on water yield in the North Esk catchment under a synthetic average climate. In this section, the model is used to simulate the water yield impact of the 50-year logging scenario in the North Esk catchment under a variable climate. Firstly, the data requirements and methodology are outlined, followed by the results.

6.2 Data and Methodology

In the previous section the impact of vegetation on water yield was investigated by removing the effect of climate variability. A synthetic climate, without interannual variability, was created by repeating the daily precipitation and temperature series of an average year (1962) for the number of years required. As noted in the introduction of the previous section, this methodology was appropriate to identify the impact of vegetation on water yield for different logging rotations, but it will not reveal the impact on water yield of vegetation changes under a variable climate.

In this section the 50-year logging scenario modelled in the previous section is re-modelled using a variable climate in order to investigate the impact on water yield of vegetation changes under a variable climate. As suggested in the previous section a variable climate could be stochastically generated to be statistically similar to the observed climate. However, this methodology would be time consuming to develop and was beyond the budget and time constraints of the current project. Instead a simple and cost-effective variable climate was developed.

The synthetic variable climate was developed by repeating the daily precipitation and temperature series for the wettest (1968), average (1962) and driest (1982) years record in the period 1950-1998. In the first, third and fifth decades of each 50-year rotation the variable climate consists of 8 years of average climate, 1 year of wet climate and 1 year of dry climate. In the second and fourth decades of each 50-year rotation the variable climate consists of 6 years of average climate, 2 consecutive years of wet climate and 2 consecutive years of dry climate. Although this synthetic variable climate is not statistically identical to the observed climate it will be similar in terms of average. This climate is more extreme than the observed climate in that the wettest and driest years occur 4 times in 50 years, rather than once in 49 years. However, this synthetic variable climate will provide a crude insight into the likely impact on water yield of vegetation changes under a variable climate. The results of this analysis are assessed using the same methods as the previous section.

6.3 Simulation results

The simulated and observed daily summary statistics of the 50-year logging scenario under a variable climate are presented in Table 6.1. Compared to the observed runoff a reduction in the mean daily flow of 2% occurs over the first rotation and a reduction in the mean daily flow of 17% occurs over the second rotation. In both rotations the variability of the daily runoff is increased by 1%.

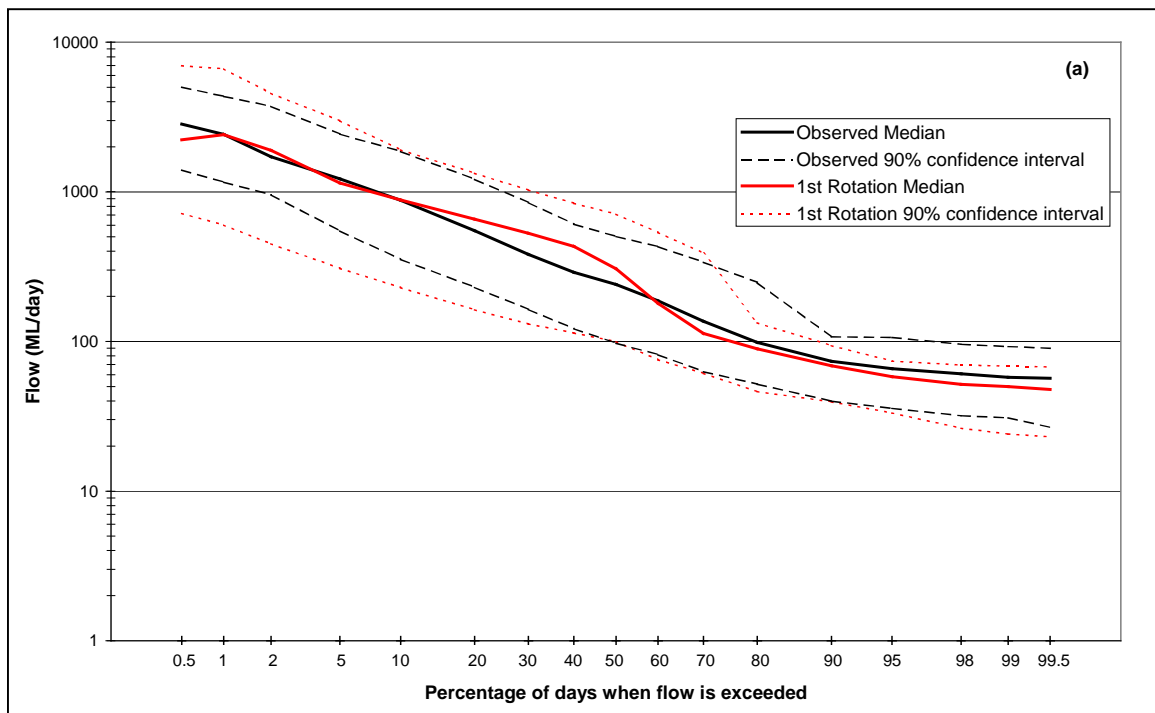
Table 6.1
Simulated and observed daily runoff summary statistics for the 50-year logging scenario.

| Variable | Period | Mean (ML) | StDev (ML) | Cv |
|----------------------------------|-----------------------|-----------|------------|------|
| Observed Daily Runoff | 1/1/1950 – 31/12/1998 | 465 | 610 | 1.31 |
| 1 st Rotation | 1/1/2010 – 31/12/2060 | 454 | 600 | 1.32 |
| 2 nd Rotation | 1/1/2061 – 31/12/2111 | 387 | 511 | 1.32 |
| % Diff Obs. 1 st Rot. | | -2% | -2% | 1% |
| % Diff Obs. 2 nd Rot. | | -17% | -16% | 1% |

The mean daily flow results in Table 6.1 are largely similar to those in Table 5.2 (same scenario under a non-varying climate). The standard deviation and coefficient of variation of daily flow in Table 6.1 are significantly higher than in Table 5.2, due to the variable climate.

The median flow duration curves and 90% confidence intervals of the simulated and observed runoff are presented in Figure 6.1. In contrast to the previous section the width of the confidence intervals is similar to the observed because the climate is variable rather than constant. The first rotation median flow duration curve is similar to the observed median curve for most of the range of probabilities of exceedance. The low flow end of the simulated median curve is just below the observed median curve. The second rotation median flow duration curve also has a similar shape to the observed median curve although it is generally lower than the observed median for most of the range of probabilities of exceedance, in particular the low flow end. The second rotation simulated median low flows are generally 23% below the observed for the lowest 40% of flows.

By using a variable, rather than average, climate in the simulations a comparison of the 90% confidence intervals is now meaningful. The simulated confidence intervals for high flows are wider than those for the observed data. However, the confidence intervals for the low flows are narrower and lower than the observed data. The wider modelled confidence intervals for high flows are due to several reasons. The first reason is that the logging rotation introduces areas of lower forest LAI than during the observed period, which results in higher flow from these areas and higher total flow. The second reason is that the recurrence of extreme wet and dry years in the synthetic climate is different (more frequent) than in the observed climate and thus the confidence intervals for modelled high flows will be wider than those for the observed period. The narrower modelled confidence intervals for low flows is mainly due to the modelled upper confidence interval being much lower than the observed, which is possibly due to the wettest year (1968) not having the wettest summer on record.



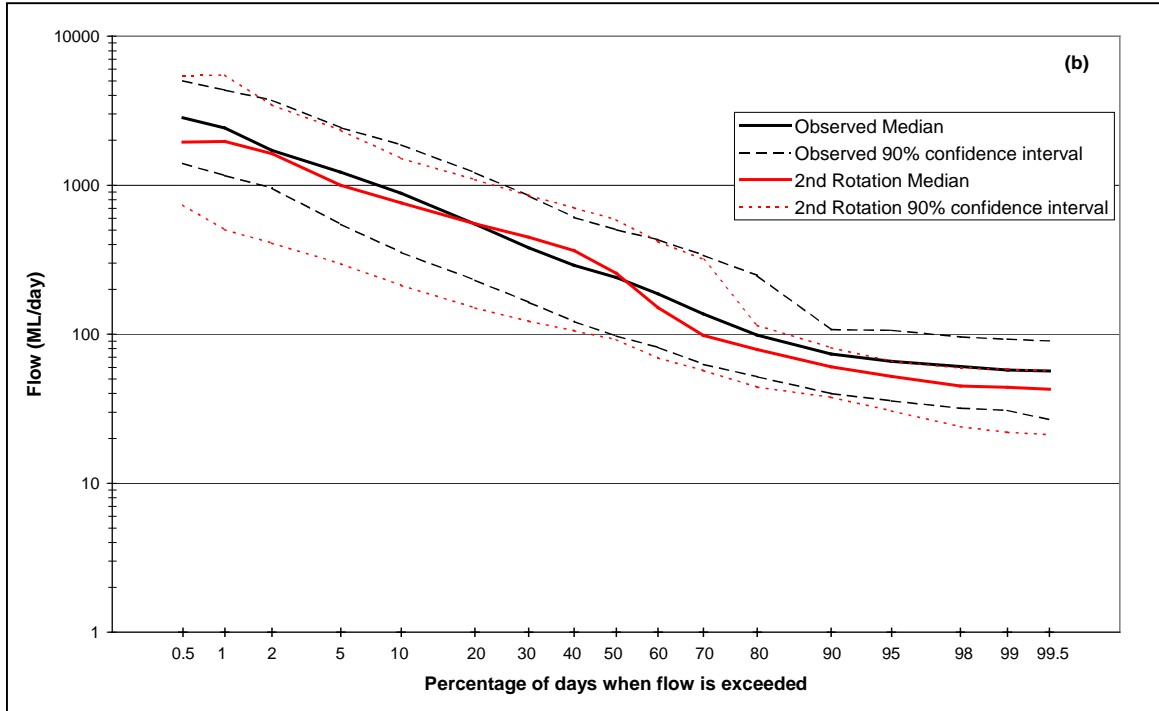


Figure 6.1 Observed and modeled median annual flow duration curves, with 90% confidence intervals for the 1st rotation (a) and 2nd rotation (b) of the 50-year rotation.

Both Table 6.1 and Figure 6.1 indicate that the impact of a 50-year logging rotation scenario in terms of mean daily flow and median flow duration curve are similar under a non-varying or varying climate. The variability of daily flow is greatly increased under the variable climate as would be expected. The modelled confidence intervals are generally wider than the observed confidence intervals except for the upper confidence interval for low flows. Generally the confidence intervals for the second rotation are lower than for the first rotation, due to the lower average age of the logged forest in the second rotation.

A summary of the impact on mean daily flow and the lowest 40% of flows is provided in Table 6.2 for the 50-year logging scenarios under both a non-varying and varying climate.

Table 6.2

Summary of the impact on mean daily flow and the lowest 40% of flows relative to the observed data for all scenarios.

| Scenario | Rotation | Mean Daily Flow (ML) | % Diff from Observed Mean Daily Flow | Average % Diff from Observed Lowest 40% of Flows |
|------------------------------|-----------------|----------------------|--------------------------------------|--|
| Observed (1950-1998) | | 465 | | |
| Calibration (1950-69) | | 480 | 3% | -12% |
| 50 Year Forest (non-varying) | 1 st | 436 | -6% | -6% |
| 50 Year Forest (non-varying) | 2 nd | 368 | -21% | -20% |
| 50 Year Forest (varying) | 1 st | 454 | -2% | -12% |
| 50 Year Forest (varying) | 2 nd | 387 | -17% | -23% |

6.4 Conclusion

Daily climate data from 1962, 1968 and 1982 was used to create a synthetic climate with crude interannual variability for use in the re-modelling of the 50-year logging scenario. Mean daily flow and median flows were similarly affected under both climates. The modelled confidence intervals are generally wider than the observed confidence intervals except for the upper confidence interval for low flows. Generally the confidence intervals for the second rotation are lower than for the first rotation, due to the lower average age of the logged forest in the second rotation.

These results indicate that the width of the flow duration confidence interval is strongly related to climate variability rather than the vegetation impact on water yield due to the 50-year logging rotation. Thus if the same variable climate were applied to the other logging rotation scenarios modelled in the previous section, it is quite likely that the width of the resultant confidence intervals would be similar to that modelled in this section. Likewise the width of modelled confidence intervals would be similar to the observed confidence intervals if a series of statistically similar stochastically generated variable climates were used for the logging rotation scenarios.

The location of the median flow duration curve and the 90% confidence interval is influenced by the vegetation changes associated with 50-year logging scenario.

7. Limitations

7.1 Introduction

There are some limitations in the accuracy of the predictions of impacts on water yield as presented. These stem from a variety of sources, including: data availability, model uncertainty, un-modelled processes, and gaps in our understanding of key tree physiological processes across a wide range of species and spatio-temporal scales. Some specific limitations are outlined below.

7.2 Data availability

The spatial and temporal accuracy of the vegetation type and age data in the North Esk catchment was a limiting factor in the accuracy of the model predictions. A more detailed map of vegetation type and age would increase the spatial and temporal accuracy of model predictions, in particular the modelling of water yield producing areas.

Detailed soils data for the North Esk were not available for this project, therefore we assumed the soil to be uniform throughout the landscape despite the fact that we know that this is not the case in the field. The Macaque model is sensitive both to the overall water holding capacity of the soil, and to its transmissivity. These properties vary with soil texture and depth.

7.3 Model uncertainty

The results of this study were sensitive to subtle variations in the response of plant water use to environmental controls relating to water availability and temperature in particular. These controls were applied within the model primarily through their influence on the conductance of leaf stomates to atmospheric humidity. The parameters values used to model this influence are uncertain, being based on one or two studies in places like the Pacific northwest of North America, and the Amazon basin; and augmented by calibrations against the expected behaviour of local forests.

7.4 Un-modelled processes

The modelling of long-term water yield, in response to forest change, hinges on the modelling of tree water use. In the present study, this was prescribed by way of some simple curves relating forest leaf area index to forest age for different species, and further curves relating maximum leaf conductance to age for all eucalypt species. These curves were derived from direct measurements as well as allometric and remote sensing data throughout the Maroondah region. However, it is likely that significant variation in LAI exists within each species, and between the Maroondah and North Esk regions. Additionally, our assumptions of leaf conductance variation with age are largely untested across a range of species. This would have a significant impact on the accurate prediction of high water yield impact areas.

8. Conclusion

In this project the process model Macaque was applied to the North Esk catchment. Spatial data describing catchment elevation, vegetation type and vegetation age and time series data for runoff, precipitation and maximum and minimum temperature were collated. The data was processed into formats suitable for Macaque.

The major aims of this project were to accurately simulate the historical streamflow record of the North Esk River (particularly the low flows) using Macaque, to investigate the source areas of low flows for the North Esk River and to assess the level of impact that changes to the distribution of vegetation age and type will have on the low flows of the North Esk River.

Macaque was successfully calibrated against runoff data for the North Esk River at the Ballroom for the period 1/1/1950 – 31/12/1969. The calibrated Macaque was also run from 1/1/1970 – 31/12/1998 as a verification of the model. The verification results indicate the possibility of unrecorded changes in the vegetation type or age in this period that was not modelled. Flow duration curves were also used to compare the observed and modelled runoff for the calibration and verification periods. The modelled lowest 40% of flows were on average 12% less than the observed for the calibration period.

Four logging rotation scenarios were simulated using a synthetic climate. The synthetic climate is daily data from a climatically average year, 1962, repeated to form a long time series. The synthetic climate has no inter-annual variability so the simulated effects on water yield are due to the modelled changes in vegetation age and species. The logging rotations modelled were 100-year, 50-year and 20-year logging rotations of areas covered in *E. regnans* and a 20-year rotation of areas covered in *E. regnans* and pasture, which was progressively converted to *E. nitens* (tree farm). Total runoff and low flows were affected least in the 100-year logging rotation scenario and most in the 20-year logging rotation and tree farm scenario. The range of mean daily flow impact of the scenarios was a reduction of 3% for the first rotation of the 20-year logging rotation to a 33% reduction for the second rotation of the 20-year logging rotation and tree farm scenario. The range of impact on the lowest 40% of flows was a 4% reduction for the first rotation of the 20-year logging rotation scenario to a 25% reduction for the 20-year logging rotation and tree farm scenario. Considering that the lowest 40% of flows were 12% lower than the observed in the calibration, the 20-year logging rotation and tree farm scenario second rotation low flows are significantly lower than the calibrated runoff.

A catchment wide fire scenario was also modelled using the synthetic climate. The maximum impact on water yield occurred eight years after the fire. The maximum impact of the fire scenario on mean daily flow was a reduction of 44% and the lowest 40% of flows were reduced by 50% relative to the observed data.

The source areas of modelled total runoff and low flows were investigated in a climatically average year. Areas covered in *E. regnans* and grassland account for 73% of the catchment area and produce 54.7% of the total runoff and 33.5% of the runoff in the three driest months (low flows). The modelled impact of the logging rotation scenarios on low flows is smaller than the modelled impact on mean daily runoff due to the modified areas of the catchment contributing a smaller proportion of runoff for low flows than for total runoff.

The potential impact on total runoff and low flows of the same logging rotation, tree farm and fire scenarios on the St Patricks catchment is likely to be similar to that modelled in the North Esk since the St Patricks catchment has a smaller area of *E. regnans* and grassland, but also a smaller area of heath and rock.

The width of the 90% flow duration curve confidence interval is strongly related to climate variability and only weakly related to vegetation changes associated with logging scenarios. However, the location of the 90% flow duration confidence interval is influenced by vegetation changes associated with logging scenarios.

The main limitation of the project was the quality of the vegetation type and vegetation age data. Several other limitations were noted but these are mainly issues for further research and model improvement.

Macaque is a relatively new catchment model that has emerged from research studies into the water balance dynamics of the Maroondah catchment. The current study represents only the fourth application of the model to a 'real-world' catchment, so caution must be exercised in interpreting the model results. Whilst we have gained more confidence in the model through the current application, we acknowledge that a lack of field data limits our ability to validate our model results.

Considering the limitations of some of the model input data, the results achieved with Macaque in this project are very good. The spatial and temporal dynamics elucidated by the model for the various logging rotation scenarios are far more detailed than any previous analyses conducted in this area of work. Most other studies of catchment response to forest logging have focused on mean annual yield impacts at a lumped catchment level. The ability of Macaque to predict responses down to the daily and Hillslope level gives catchment managers considerable insight into how different logging regimes would impact on water resources in different ways.

9. References

- Baret F, Olioso A, Luciani JL & Hanocq JF, 1989, Estimation de l'énergie photosynthétiquement active absorbée par une culture de blé à partir de données radiométriques. *Agronomie*, **9**:885-895.
- Beven KJ, Lamb R, Quinn P, Romanowicz R & Freer J, 1995, TOPMODEL. In: Singh VP (ed.), *Computer Models of Watershed Hydrology*, Water Resources Publications, Highland Ranch, Colorado, 627-668.
- Chiew FHS, Stewardson MJ & McMahon TA, 1993, Comparison of six rainfall-runoff modelling approaches. *Journal of Hydrology*, **147**:1-36.
- Kuczera G, 1987, Prediction of water yield reductions following a bushfire in ash-mixed species eucalypt forest. *Journal of Hydrology*, **94**:215-236.
- Lacaze B, 1996, Spectral characterization of vegetation communities and practical approaches to vegetation cover changes monitoring. *Remote Sensing for Land Degradation and Desertification Monitoring in the Mediterranean Basin*, Workshop Proceedings, Valencia, 13-15 June 1994, in press.
- McClenaghan MP & Calver CR (comp.), 1994, Geological Atlas 1:250000 digital series. Geology of Northeast Tasmania. Tasmanian Geological Survey.
- Monteith JL & Unsworth MH, 1990, *Principles of Environmental Physics* (2nd ed.). Routledge, Chapman & Hall, New York, 291pp.
- Nash JE & Sutcliffe JV, 1970, River flow forecasting through conceptual models, 1. A discussion of principles. *Journal of Hydrology*, **10**:282-290.
- Parrish RS, 1990, Comparison of quantile estimators in normal sampling. *Biometrics*, **46**: 247-257.
- Peel MC, 1999, Annual runoff variability in a global context. PhD thesis, Dept. of Geography and Environmental Studies, The University of Melbourne, Australia.
- Peel MC, Watson FGR, Vertessy RA, Lau JA, Watson IS, Sutton MW & Rhodes BG, 2000, Predicting the water yield impacts of forest disturbance in the Maroondah and Thomson catchments using the Macaque model. Technical Report 00/14, The Cooperative Research Centre for Catchment Hydrology, Melbourne, Australia.
- Rawls WJ, Ahuja LR, Brakensiek DL & Shirmohammadi A, 1993, Infiltration and soil water movement, In: Maidment DR (ed.), *Handbook of Hydrology*, McGraw-Hill, New York, 5.1-5.51.
- Roberts SL, Vertessy RA, Grayson RG, 2001. Transpiration from *Eucalyptus sieberi* (L. Johnson) forests of different age. *Forest Ecology and Management*, **143**:153-161.
- Rouse JW, Haas RH, Schell JA & Deering DW, 1973, Monitoring vegetation systems in the great plains with ERTS. Third ERTS Symposium, Vol. 1.
- Rouse JW, Haas RH, Schell JA, Deering DW & Harlan JC, 1974, Monitoring the vernal advancement and retrogradation (greenwave effect) of natural vegetation. NASA/GSFC Type III Final Report, Greenbelt, Maryland, USA.
- Shaw EM, 1994, *Hydrology in Practice*, Chapman & Hall, London
- Van Genuchten MT, 1980, A closed-form equation for predicting the hydraulic conductivity of unsaturated soil. *Soil Sci. Soc. Am. J.*, **44**:892-898.
- Vertessy RA, Benyon R & Haydon S, 1994, Melbourne's forest catchments: effect of age on water yield. *Water*, **21**: 17-20.

Vertessy RA, Watson FGR, O'Sullivan SK, Davis S & Benyon R, 1998, Predicting water yield from mountain ash forest catchments. Cooperative research Centre for Catchment Hydrology, Melbourne, Industry Report, 98/4, 38pp.

Vertessy RA, Watson FGR & O'Sullivan SK, 2001, Factors determining relations between stand age and catchment water balance in mountain ash forests. *Forest Ecology and Management*, **143**:13-26.

Vogel RM & Fennessey NM, 1994, Flow-Duration Curves. 1: New Interpretation and confidence intervals. *Journal of Water Resources Planning and Management*, **120**(4):485-504.

Watson FGR, 1999, Large scale, long term modelling of the effects of land cover change on forest water yield. PhD thesis, Dept. of Civil and Environmental Eng., The University of Melbourne, Australia.

Watson FGR, 2000, Tarsier. <http://earthsystems.monterey.edu/~fwatson/tarsier.html>.

Watson FGR, Grayson RB, Vertessy RA & McMahon TA, 1998, Large-scale distribution modelling and the utility of detailed ground data. *Hydrological Processes*, **12**:873-888.

Watson FGR, Vertessy RA, McMahon TA, Rhodes BG & Watson IS, 1999a, The hydrologic impacts of forestry on the Maroondah catchments. Cooperative research Centre for Catchment Hydrology, Melbourne, Report 99/1, 80pp.

Watson FGR, Vertessy RA & Grayson RB, 1999b, Large-scale modelling of forest hydrological processes and their long-term effect on water yield. *Hydrological Processes*, **13**:689-700.

Watson FGR, Grayson RB, Vertessy RA, Peel MC & Pierce LL, 2001, Evolution of a Hillslope Hydrologic Model. In MODSIM 2001 – International Congress on Modelling and Simulation, Canberra, December 2001, pp: 461-467.

A. Appendix (Flow duration curve values)

The flow duration curves presented in Sections 4 and 5 provide a visual assessment of the calibration, verification and scenario results. The tables in this appendix contain the raw data used to construct those flow duration curves. Each table (except the catchment wide fire scenario) contains the daily flow (in ML) for the given range of probabilities of exceedance for the median (50%) and the 90% confidence interval (95% and 5%). The catchment wide fire scenario contains the daily flow for the given range of probabilities of exceedance for the median only.

Table A.1 Flow duration values (in ML) for the observed data (1950-1998).

| | 0.5% | 1% | 2% | 5% | 10% | 50% | 90% | 95% | 98% | 99% | 99.5% |
|-----|------|------|------|------|------|-----|-----|-----|-----|-----|-------|
| 95% | 5019 | 4347 | 3730 | 2436 | 1866 | 504 | 108 | 106 | 96 | 92 | 90 |
| 50% | 2837 | 2419 | 1718 | 1225 | 880 | 240 | 73 | 66 | 61 | 58 | 57 |
| 5% | 1397 | 1161 | 958 | 548 | 354 | 97 | 40 | 36 | 32 | 31 | 27 |

Table A.2 Flow duration values (in ML) for the calibrated data (1950-1969).

| | 0.5% | 1% | 2% | 5% | 10% | 50% | 90% | 95% | 98% | 99% | 99.5% |
|-----|------|------|------|------|------|-----|-----|-----|-----|-----|-------|
| 95% | 7087 | 5742 | 4028 | 2645 | 1783 | 654 | 195 | 171 | 155 | 140 | 132 |
| 50% | 2996 | 2275 | 1921 | 1271 | 834 | 280 | 62 | 53 | 49 | 47 | 46 |
| 5% | 918 | 787 | 637 | 303 | 181 | 83 | 15 | 12 | 10 | 9 | 9 |

Table A.3 Flow duration values (in ML) for the verification data (1970-1998).

| | 0.5% | 1% | 2% | 5% | 10% | 50% | 90% | 95% | 98% | 99% | 99.5% |
|-----|------|------|------|------|------|-----|-----|-----|-----|-----|-------|
| 95% | 7154 | 5384 | 3319 | 1910 | 1265 | 540 | 133 | 112 | 92 | 87 | 82 |
| 50% | 1972 | 1409 | 1158 | 850 | 640 | 199 | 56 | 45 | 39 | 36 | 36 |
| 5% | 669 | 610 | 432 | 290 | 222 | 107 | 25 | 18 | 16 | 16 | 15 |

Table A.4 Flow duration values (in ML) for the 100 Year Forest scenario 1st rotation.

| | 0.5% | 1% | 2% | 5% | 10% | 50% | 90% | 95% | 98% | 99% | 99.5% |
|-----|------|------|------|------|-----|-----|-----|-----|-----|-----|-------|
| 95% | 2816 | 2580 | 2086 | 1291 | 997 | 345 | 76 | 65 | 59 | 58 | 57 |
| 50% | 2334 | 2436 | 1915 | 1186 | 905 | 319 | 74 | 62 | 55 | 54 | 53 |
| 5% | 2086 | 1945 | 1684 | 1029 | 786 | 272 | 67 | 57 | 50 | 50 | 48 |

Table A.5 Flow duration values (in ML) for the 100 Year Forest scenario 2nd rotation.

| | 0.5% | 1% | 2% | 5% | 10% | 50% | 90% | 95% | 98% | 99% | 99.5% |
|-----|------|------|------|------|-----|-----|-----|-----|-----|-----|-------|
| 95% | 2466 | 2244 | 1802 | 1129 | 834 | 286 | 68 | 60 | 52 | 51 | 50 |
| 50% | 2267 | 2054 | 1738 | 1085 | 805 | 277 | 66 | 58 | 50 | 49 | 48 |
| 5% | 1982 | 1905 | 1672 | 1017 | 773 | 262 | 62 | 54 | 47 | 46 | 45 |

Table A.6 Flow duration values (in ML) for the 50 Year Forest scenario 1st rotation.

| | 0.5% | 1% | 2% | 5% | 10% | 50% | 90% | 95% | 98% | 99% | 99.5% |
|-----|------|------|------|------|-----|-----|-----|-----|-----|-----|-------|
| 95% | 2784 | 2611 | 2087 | 1291 | 993 | 345 | 75 | 63 | 57 | 56 | 55 |
| 50% | 2276 | 2432 | 1931 | 1186 | 918 | 320 | 73 | 61 | 55 | 54 | 52 |
| 5% | 1887 | 2117 | 1665 | 1014 | 746 | 246 | 59 | 51 | 45 | 44 | 42 |

Table A.7 Flow duration values (in ML) for the 50 Year Forest scenario 2nd rotation.

| | 0.5% | 1% | 2% | 5% | 10% | 50% | 90% | 95% | 98% | 99% | 99.5% |
|-----|------|------|------|------|-----|-----|-----|-----|-----|-----|-------|
| 95% | 2275 | 2153 | 1700 | 1084 | 786 | 269 | 65 | 57 | 50 | 49 | 47 |
| 50% | 2141 | 1969 | 1650 | 1016 | 764 | 258 | 62 | 53 | 47 | 46 | 45 |
| 5% | 1827 | 1894 | 1571 | 940 | 714 | 239 | 57 | 50 | 44 | 43 | 42 |

Table A.8 Flow duration values (in ML) for the 20 Year Forest scenario 1st rotation.

| | 0.5% | 1% | 2% | 5% | 10% | 50% | 90% | 95% | 98% | 99% | 99.5% |
|-----|------|------|------|------|------|-----|-----|-----|-----|-----|-------|
| 95% | 2843 | 2631 | 2107 | 1325 | 1013 | 357 | 79 | 68 | 61 | 59 | 58 |
| 50% | 2268 | 2473 | 1959 | 1222 | 938 | 329 | 75 | 63 | 57 | 56 | 54 |
| 5% | 1809 | 2183 | 1741 | 1065 | 746 | 247 | 60 | 51 | 45 | 44 | 43 |

Table A.9 Flow duration values (in ML) for the 20 Year Forest scenario 2nd rotation.

| | 0.5% | 1% | 2% | 5% | 10% | 50% | 90% | 95% | 98% | 99% | 99.5% |
|-----|------|------|------|------|-----|-----|-----|-----|-----|-----|-------|
| 95% | 2337 | 2283 | 1754 | 1103 | 825 | 282 | 69 | 62 | 54 | 53 | 51 |
| 50% | 2076 | 2065 | 1644 | 1030 | 772 | 257 | 61 | 53 | 46 | 46 | 44 |
| 5% | 1887 | 1908 | 1491 | 924 | 704 | 235 | 56 | 49 | 43 | 42 | 41 |

Table A.10 Flow duration values (in ML) for the 20 Year Forest and Tree Farm scenario 1st rotation.

| | 0.5% | 1% | 2% | 5% | 10% | 50% | 90% | 95% | 98% | 99% | 99.5% |
|-----|------|------|------|------|------|-----|-----|-----|-----|-----|-------|
| 95% | 2841 | 2664 | 2110 | 1326 | 1012 | 357 | 79 | 68 | 61 | 59 | 58 |
| 50% | 2244 | 2450 | 1948 | 1218 | 942 | 329 | 75 | 63 | 57 | 56 | 54 |
| 5% | 1835 | 1419 | 1206 | 771 | 572 | 211 | 57 | 47 | 43 | 43 | 42 |

Table A.11 Flow duration values (in ML) for the 20 Year Forest and Tree Farm scenario 2nd rotation.

| | 0.5% | 1% | 2% | 5% | 10% | 50% | 90% | 95% | 98% | 99% | 99.5% |
|-----|------|------|------|-----|-----|-----|-----|-----|-----|-----|-------|
| 95% | 2323 | 1757 | 1495 | 920 | 700 | 256 | 67 | 59 | 53 | 52 | 50 |
| 50% | 2059 | 1527 | 1300 | 819 | 627 | 227 | 59 | 50 | 45 | 45 | 43 |
| 5% | 1792 | 1356 | 1219 | 741 | 566 | 207 | 55 | 46 | 42 | 41 | 40 |

Table A.12 Flow duration values (in ML) for the catchment wide fire scenario maximum impact.

| | 0.5% | 1% | 2% | 5% | 10% | 50% | 90% | 95% | 98% | 99% | 99.5% |
|-----|------|------|------|-----|-----|-----|-----|-----|-----|-----|-------|
| 50% | 2328 | 1848 | 1306 | 733 | 524 | 171 | 39 | 32 | 29 | 29 | 23 |

Table A.13 Flow duration values (in ML) for the 50 Year Forest scenario 1st rotation under a variable climate.

| | 0.5% | 1% | 2% | 5% | 10% | 50% | 90% | 95% | 98% | 99% | 99.5% |
|-----|------|------|------|------|------|-----|-----|-----|-----|-----|-------|
| 95% | 6967 | 6636 | 4554 | 2985 | 1905 | 709 | 94 | 74 | 70 | 68 | 68 |
| 50% | 2233 | 2402 | 1898 | 1149 | 884 | 307 | 69 | 58 | 52 | 50 | 48 |
| 5% | 718 | 599 | 449 | 308 | 230 | 100 | 39 | 33 | 26 | 24 | 23 |

Table A.14 Flow duration values (in ML) for the 50 Year Forest scenario 2nd rotation under a variable climate.

| | 0.5% | 1% | 2% | 5% | 10% | 50% | 90% | 95% | 98% | 99% | 99.5% |
|-----|------|------|------|------|------|-----|-----|-----|-----|-----|-------|
| 95% | 5422 | 5482 | 3452 | 2335 | 1512 | 586 | 81 | 66 | 59 | 58 | 57 |
| 50% | 1952 | 1967 | 1627 | 1001 | 761 | 256 | 61 | 52 | 45 | 44 | 43 |
| 5% | 738 | 504 | 409 | 297 | 213 | 92 | 38 | 31 | 24 | 22 | 21 |

B. Appendix (Species annual evapotranspiration)

Annual evapotranspiration from species modelled in the North Esk catchment is summarised by depth and volume for the climatically average (1962) simulation (Section 5.4) and the 2nd rotation of the 20-year logging and tree-farming scenario (Section 5.3). The species modelled relate to the original vegetation types provided by Forestry Tasmania as described in Section 3.3.2. The results for *E. obliqua*, *Acacia dealbata*, *Nothofagus*, heath and rocky are the same for both simulations and are thus not repeated. In the 2nd rotation of the 20-year logging and tree-farming scenario all the grassland has been converted to tree farm and tree farm regrowth is being logged and replanted. The annual volumes in Table B.1 are in Megaliters (ML) and are for the total area covered by the relevant specie.

Table B.1 Annual depths (mm) and volumes (ML) of precipitation (P), runoff (R) and evapotranspiration (ET) for the different species modelled in the North Esk catchment for the climatically average (1962) simulation and the 2nd rotation of the 20-year logging and tree-farming scenario.

| Species | Area (ha) | P (mm) | R (mm) | ET (mm) | P (ML) | R (ML) | ET (ML) |
|--|-----------|--------|--------|---------|--------|--------|---------|
| Climatically average (1962) | | | | | | | |
| <i>E. regnans</i> (150 years old) | 22504 | 1262 | 275 | 987 | 284000 | 61886 | 222114 |
| Grassland | 4342 | 1200 | 686 | 514 | 52104 | 29786 | 22318 |
| <i>E. obliqua</i> | 6579 | 1392 | 656 | 736 | 91580 | 43158 | 48421 |
| <i>Acacia dealbata</i> | 587 | 1261 | 294 | 967 | 7402 | 1726 | 5676 |
| <i>Nothofagus</i> | 944 | 1306 | 298 | 1008 | 12329 | 2813 | 9516 |
| Heath | 1136 | 2136 | 1729 | 407 | 24265 | 19641 | 4624 |
| Rocky | 638 | 1676 | 1381 | 295 | 10693 | 8811 | 1882 |
| Total | 36730 | 1313 | 457 | 856 | 482373 | 167821 | 314551 |
| 2nd rotation of the 20-year logging & tree-farming | | | | | | | |
| <i>E. regnans</i> (10 years old) | 22504 | 1262 | 86 | 1176 | 284000 | 19353 | 264647 |
| Tree Farm (10 years old) | 4342 | 1200 | 166 | 1034 | 52104 | 7208 | 44896 |